Communications on Applied Mathematics and Computation
https://doi.org/10.1007/s42967-021-00130-9

ORIGINAL PAPER

Dual-Wind Discontinuous Galerkin Methods for Stationary Hamilton-Jacobi Equations and Regularized Hamilton-Jacobi Equations

Xiaobing Feng[1] · **Thomas Lewis**[2] · **Aaron Rapp**[3]

Received: 3 September 2020 / Revised: 30 January 2021 / Accepted: 5 March 2021

Abstract
This paper develops and analyzes a new family of dual-wind discontinuous Galerkin (DG) methods for stationary Hamilton-Jacobi equations and their vanishing viscosity regularizations. The new DG methods are designed using the DG finite element discrete calculus framework of [17] that defines discrete differential operators to replace continuous differential operators when discretizing a partial differential equation (PDE). The proposed methods, which are non-monotone, utilize a dual-winding methodology and a new skew-symmetric DG derivative operator that, when combined, eliminate the need for choosing indeterminable penalty constants. The relationship between these new methods and the local DG methods proposed in [38] for Hamilton-Jacobi equations as well as the generalized-monotone finite difference methods proposed in [13] and corresponding DG methods proposed in [12] for fully nonlinear second order PDEs is also examined. Admissibility and stability are established for the proposed dual-wind DG methods. The stability results are shown to hold independent of the scaling of the stabilizer allowing for choices that go beyond the Godunov barrier for monotone schemes. Numerical experiments are provided to gauge the performance of the new methods.

Keywords Hamilton-Jacobi equations · Discontinuous Galerkin methods · Vanishing viscosity method

X. Feng: The work of this author was partially supported by the NSF Grant DMS-1620168.

✉ Xiaobing Feng
xfeng@utk.edu

Thomas Lewis
tllewis3@uncg.edu

Aaron Rapp
aaron.rapp@uvi.edu

[1] Department of Mathematics, The University of Tennessee, Knoxville, TN 37996, USA

[2] Department of Mathematics and Statistics, The University of North Carolina at Greensboro, Greensboro, NC 27402, USA

[3] Department of Mathematical Sciences, University of the Virgin Islands, Kingshill, USVI 00850-9781, US Virgin Islands

Published online: 19 June 2021

Mathematics Subject Classification 65N30

1 Introduction

Let $\Omega \subset \mathbb{R}^d$ $(d = 1, 2, 3)$ be a bounded convex polygonal domain. We consider the following stationary Hamilton-Jacobi (HJ) equation with the Dirichlet boundary condition:

$$\mathcal{H}^0[u] \equiv \mathcal{H}(\nabla u, u, x) + \theta u = 0 \qquad \text{in } \Omega, \tag{1a}$$

$$u = g \quad \text{on } \partial\Omega, \tag{1b}$$

where $\theta \geqslant 0$ is a constant, $g \in C^0(\partial\Omega)$, and $\mathcal{H} : \mathbb{R}^d \times \mathbb{R} \times \Omega \to \mathbb{R}$ with $(\mathbf{v}, v, x) \to \mathcal{H}(\mathbf{v}, v, x)$ is continuous with respect to $x \in \Omega$, globally Lipschitz with respect to $\mathbf{v} \in \mathbb{R}^d$ and $v \in \mathbb{R}$, and nondecreasing with respect to v. We also consider the vanishing viscosity regularization of (1) defined by

$$\mathcal{H}^\sigma[u] \equiv -\sigma\Delta u + \mathcal{H}(\nabla u, u, x) + \theta u = 0 \qquad \text{in } \Omega, \tag{2a}$$

$$u = g \quad \text{on } \partial\Omega \tag{2b}$$

for $\sigma > 0$, which is a proper elliptic second order problem. With appropriate assumptions for $\mathcal{H}^\sigma$, the solution u^σ of (2) exists and $u^\sigma \to v$ in $L^\infty(\Omega)$ at a rate of $\mathcal{O}(\sqrt{\sigma})$ with v the viscosity solution to (1) (see [27]). The function u^σ is often called the vanishing viscosity approximation of the limit function v for small σ. See Sect. 2.1 for a more detailed discussion regarding viscosity solutions and the existence and uniqueness theory for (1) and (2) as well as how the boundary condition must be interpreted.

HJ equations arise from many scientific applications including optimal control, wave propagation, geometric optics, multiphase flow, image processing, etc. (cf. [28, 31] and the references therein). Their numerical approximations have been vital in understanding solutions to the application problems. There has been significant progress for approximating (1) and (2) as well as the related time-dependent problems (cf. [3, 7, 9, 18, 19, 21, 29, 32–34, 36] and the references therein). Monotone finite difference (FD) methods and associated finite volume methods have been proven to converge to the viscosity solution of (1) and (2) when viewing them as fully nonlinear elliptic problems (see [2]) expanding the earlier results of Crandall and Lions in [9] for HJ equations. Standard examples of convergent monotone FD methods that form the basis for many other methods are the Lax-Friedrich's and Godunov methods borrowed from the approximation theory for nonlinear hyperbolic conservations laws (see [35]). Unfortunately, all monotone methods are limited to first-order accuracy due to the Godunov barrier (see [34]). Consequently, in order to achieve high order, non-monotone schemes must be used.

To overcome the Godunov barrier, several formal approaches have been used to design high-order methods; see [3, 33] and the references therein for some earlier works. Recently, the central discontinuous Galerkin (DG) method proposed by Li and Yakovlev in [26] and the positivity preserving local DG (LDG) method by van der Vegt et al. in [37] adapted slope-limiters and other techniques successfully used for solving hyperbolic equations to HJ equations. Such methods use ideas from high order essentially nonoscillatory schemes and weighted nonoscillatory schemes to motivate the stabilization and time stepping for approximating time-dependent HJ equations. Going further, Yan and Osher proposed in

[38] a general LDG framework which allows for the utilization of any numerical viscosity technique (such as Lax-Friedrich's and Godunov's numerical Hamiltonians) designed for hyperbolic conservation laws to construct LDG methods for time-dependent HJ equations. It should be noted that all of these works were geared towards time-dependent HJ equations where time-stepping plays an essential role; their applicability and analyses for stationary HJ equations (if it is possible) are far from straightforward.

The goals of this paper are to formulate DG methods for approximating both (1) and (2) and to develop analysis techniques that focus on admissibility and stability results as a first step towards a complete convergence analysis framework for analyzing DG methods that directly approximate the viscosity solution of (1). The proposed methods formally have optimal consistency errors in both the L^2 and H^1-norm. When compared to the time-dependent counterpart of (1) discretized by appropriate time-stepping schemes, the stationary problem (1) has some inherent difficulties in establishing the admissibility and stability analysis for any approximation method. In contrast, the regularized problem (2) is easier in the sense that the extra viscous term for a fixed $\sigma > 0$ can help to control discrete "convection" terms when the mesh size is sufficiently small. However, when viewing (2) as a viscosity approximation to (1), the need to allow the mesh to resolve the viscosity term will add a contribution to the global consistency error. The techniques in this paper also provide a new approach for analyzing the admissibility and stability of other dynamic methods when adapted to the stationary problem.

We focus on non-monotone dual-wind discontinuous Galerkin (DWDG) methods based on the DG discrete differential calculus developed in [17]. As DG methods were first designed for conservation laws and are known to be highly accurate and efficient, adopting DG methods to HJ equations is a natural approach for designing high order methods. The DG discrete calculus provides a systematic and flexible way to approximate ∇u and design approximation methods for (1) where multiplication by a test function and integration by parts does not apply. The DG calculus helps with designing a skew-symmetric gradient approximation that is the key to eliminating the need for carefully choosing upwind fluxes as is typically the focus for FD and finite element (FE) approximations of reaction-convection-diffusion problems. The DWDG idea was first used in [23] to solve Poisson problems. The method utilizes the discrete derivative operators from the DG discrete calculus to define a symmetric approximation for the Laplacian operator Δ that is L^2-stable and naturally enforces boundary conditions without adding additional stabilization terms. The systematic approach of the DWDG method also avoids the need to introduce interior and/or boundary penalty terms typically needed in DG methods for stationary elliptic problems. Thus, the DWDG approach offers a natural candidate for discretizing (2) without introducing stabilization and penalty terms, and it can be used in (1) by choosing parameters $\sigma_h \to 0$ at high order in (2). The DWDG method also provides a prototypical example for developing the new analytic techniques for stationary problems which could be extended to other methods because the relationships between DWDG and stabilization techniques for other DG methods have already been established.

We also note that when $\mathcal{H}$ is linear, (2) reduces to a linear reaction-convection-diffusion problem. Standard finite element approximations of (2) are known to produce spurious oscillations for convection-dominated problems unless the mesh parameter h is small enough compared to σ. Typically, a stabilization term in the upwind/streamline direction is introduced to combat this issue as discussed in [1, 5, 7, 20] and the references therein. However, unlike convection-diffusion equations, the upwind directions associated with the nonlinear operator $\mathcal{H}$ may not be as clearly defined. As a by product, the DG methods of this paper when applied to linear convection-diffusion problems do not require tuning

stabilization terms, enriching the piecewise polynomial space, or implementing rules to ensure the fluxes are chosen to match the nonlinear convection.

The remainder of this paper is organized as follows. In Sect. 2 we introduce some preliminaries which include the space notation and structure assumptions, some background for viscosity solutions, the notation from the DG differential calculus, and the DG derivative operators to be used to define our DWDG methods for (1) and (2). In Sect. 3 we formulate our DWDG methods. Section 4 is devoted to proving the existence, uniqueness, and L^2-stability of the proposed DWDG methods. Several 2D numerical tests are presented in Sect. 5 to gauge the accuracy and efficiency of the proposed DWDG methods. Finally, we mention some possible extensions in Sect. 6 to other DG schemes and make some concluding remarks in Sect. 7.

2 Preliminaries

Standard space notation will be adopted in this paper (cf. [4, 6]). The notation and definitions for the DG derivative operators are borrowed from [11, 12, 17, 23]. Throughout the paper, κ will be used to denote a Lipschitz constant for $\mathcal{H}$ where

$$|\mathcal{H}(\mathbf{v}, v, x) - \mathcal{H}(\mathbf{w}, w, x)| \leqslant \kappa \max\left\{\|\mathbf{v} - \mathbf{w}\|_{\ell^\infty}, |v - w|\right\}, \qquad \forall \mathbf{v}, \mathbf{w} \in \mathbb{R}^d, \qquad \forall v, w \in \mathbb{R} \tag{3}$$

for all $x \in \Omega$. Since $\mathcal{H}(\mathbf{v}, v, x)$ is assumed to be nondecreasing with respect to v, there exists $\kappa_0 \geqslant 0$ such that

$$\frac{\mathcal{H}(\mathbf{v}, v, x) - \mathcal{H}(\mathbf{v}, w, x)}{v - w} \geqslant \kappa_0, \qquad \forall v > w,\ \mathbf{v} \in \mathbb{R}^d,\ x \in \Omega. \tag{4}$$

For clarity, we shall distinguish between the non-degenerate case when $\max\{\kappa_0, \theta\} > 0$ and the degenerate case when $\theta = \kappa_0 = 0$.

2.1 Viscosity Solutions

In this section we recall the concept of viscosity solutions and record the relationship between u solving (1) and u^σ solving (2) as well as how the boundary condition is interpreted in (1). Indeed, by the method of characteristics, the boundary condition in (1) should only be enforced on the inflow boundary. When specifying the boundary condition over the entire boundary $\partial\Omega$, the boundary condition can only be satisfied in the "viscosity sense" to account for any incompatibilities with the boundary data. The results in this section are based on results found in [27].

In general, classical solutions do not exist for (1). Instead, generalized solutions are defined that are typically locally Lipschitz over Ω and continuous over $\overline{\Omega}$. Thus, the generalized solutions satisfy (1) almost everywhere by Rademacher's theorem. Unfortunately, there may exist infinitely many generalized solutions for (1). Therefore, we focus on a special class of generalized solutions called viscosity solutions.

Sufficient conditions for the Dirichlet problem (1) to have such a viscosity solution are

(i) $\mathcal{H}(\mathbf{v}, v, \cdot) \to \infty$ as $|\mathbf{v}| \to \infty$ and $\mathcal{H}(\mathbf{v}, v, \cdot)$ is nondecreasing in v; and
(ii) there exists $v \in C^1(\Omega) \cap C(\overline{\Omega})$ such that $\mathcal{H}^0(\nabla v, v, x) \leqslant 0$ in Ω and $v = g$ on $\partial\Omega$.

If $\mathcal{H}^0$ is convex, then it is sufficient to have $v \in W^{1,\infty}(\Omega)$ and $\mathcal{H}^0(\nabla v, v, x) \leqslant 0$ almost everywhere in Ω with $v = g$ on $\partial\Omega$ in (ii). Convexity with respect to ∇v also guarantees the uniqueness. Property (i) ensures the problem is nonlinear.

Since we are assuming both $\mathcal{H}$ and g are continuous in (1) and (2), we have the following definition of a viscosity solution that satisfies the boundary condition in the viscosity sense:

Definition 1 Let $\mathcal{H}^\sigma$ denote the differential operator in (1) or (2) for $\sigma \geqslant 0$, and let g denote the boundary value.

i) A function $u \in C(\overline{\Omega})$ is called a *viscosity subsolution* of (1) for $\sigma = 0$ or (2) for $\sigma > 0$ if $\forall \varphi \in C^2(\overline{\Omega})$, when $u - \varphi$ has a local maximum at $x_0 \in \overline{\Omega}$ with $u(x_0) = \varphi(x_0)$, there holds $\mathcal{H}^\sigma[\varphi](x_0) \leqslant 0$ if $x_0 \in \Omega$ or there holds $\min\left\{u(x_0) - g(x_0), \mathcal{H}^\sigma[\varphi](x_0)\right\} \leqslant 0$ if $x_0 \in \partial\Omega$.
ii) A function $u \in C(\overline{\Omega})$ is called a *viscosity supersolution* of (1) for $\sigma = 0$ or (2) for $\sigma > 0$ if $\forall \varphi \in C^2(\overline{\Omega})$, when $u - \varphi$ has a local minimum at $x_0 \in \overline{\Omega}$ with $u(x_0) = \varphi(x_0)$, there holds $\mathcal{H}^\sigma[\varphi](x_0) \geqslant 0$ if $x_0 \in \Omega$ or $\max\left\{u(x_0) - g(x_0), \mathcal{H}^\sigma[\varphi](x_0)\right\} \geqslant 0$ if $x_0 \in \partial\Omega$.
iii) A function $u \in C(\overline{\Omega})$ is called a *viscosity solution* of (1) for $\sigma = 0$ or (2) for $\sigma > 0$ if u is both a viscosity subsolution and a viscosity supersolution of the problem.

Remark 1 The definition is a newer interpretation than in the original works of Crandall and Lions since it combines the definition with second order PDEs (see [10]). When $\sigma = 0$, we can assume $\varphi \in C^1(\overline{\Omega})$.

The above definition is equivalent to the constructive approach that defines the viscosity solution of (1) as the limit of the regularized solutions u^σ of (2). When the boundary condition g is incompatible with $\mathcal{H}^0$ so that $u \neq g$ on $\partial\Omega$, then u^σ converges locally to a solution of (1) but with a different boundary condition. This boundary value is the one which is satisfied both in the viscosity sense and in the pointwise sense. The inconsistency in the formulation for u^σ based on the incompatible boundary data g leads to a boundary layer in the convergence of u^σ to the viscosity solution u.

Suppose $\mathcal{H} : \mathbb{R}^d \times \Omega \to \mathbb{R}$ with $(\mathbf{v}, x) \to \mathcal{H}(\mathbf{v}, x)$. Then, standard L^∞ stability bounds for the viscosity solution u are inversely related to θ in the definition of $\mathcal{H}^0$. Thus, the case when $\theta = 0$ requires more care. If $\mathcal{H}^0(\mathbf{v}, v, x)$ is non-decreasing with respect to v for all $(\mathbf{v}, x) \in \mathbb{R}^d \times \overline{\Omega}$ and there exists $v_0 \in \mathbb{R}$ such that $\mathcal{H}^0(\mathbf{0}, v_0, x) \geqslant \alpha > 0$ for all $x \in \overline{\Omega}$ for some $\alpha > 0$, then, the stability can be shown to hold even for $\theta = 0$.

2.2 DG Notation

Let $\mathcal{T}_h$ denote a shape-regular simplicial triangulation of Ω [4, 6]. Set $\mathcal{E}_h^{\mathrm{I}}$ to be the set of interior $(d-1)$-dimensional simplices in the triangulation, $\mathcal{E}_h^{\mathrm{B}}$ the set of boundary $(d-1)$-dimensional simplices, and $\mathcal{E}_h \equiv \mathcal{E}_h^{\mathrm{I}} \cup \mathcal{E}_h^{\mathrm{B}}$. The parameter h_K denotes the diameter of the simplex $K \in \mathcal{T}_h$, and we define $h \equiv \max_{K \in \mathcal{T}_h} h_K$. Lastly, we define h_e to be the diameter of $e \in \mathcal{E}_h$.

The piecewise L^2 inner product with respect to the triangulation is given by $(v, w)_{\mathcal{T}_h} \equiv \sum_{K \in \mathcal{T}_h} \int_K vw \, \mathrm{d}x$, and the piecewise L^2 inner product over a subset $\mathcal{S}_h \subset \mathcal{E}_h$ is given by $\left\langle v, w \right\rangle_{\mathcal{S}_h} \equiv \sum_{e \in \mathcal{S}_h} \int_e vw \, \mathrm{d}s$. We denote the L^2 norm over the triangularization by

$\|v\|^2_{L^2(\mathcal{T}_h)} \equiv (v,v)_{\mathcal{T}_h}$. Lastly, we define the piecewise vector space with respect to the triangulation $\mathcal{V}_h \equiv \left\{v : v\big|_K \in W^{1,1}(K) \cap C^0(K) \text{ for all } K \in \mathcal{T}_h\right\}$, where $W^{m,p}(K)$ denotes the set of all $L^p(\Omega)$ functions whose distributional derivatives up to order m are in $L^p(K)$.

For an integer $r \geqslant 1$, we let V_h^r denote the space of piecewise polynomials of degree less than or equal to r with respect to the triangulation $\mathcal{T}_h$; that is, $V_h^r = \left\{v : v\big|_K \in \mathcal{P}_r(K) \text{ for all } K \in \mathcal{T}_h\right\}$, where $\mathcal{P}_r(K)$ denotes the space of polynomials with domain K and degree not exceeding r. Note that $V_h^r \subset \mathcal{V}_h$. We also define the vector-valued DG space $\mathbf{V}_h^r$ by $\mathbf{V}_h^r \equiv \left[V_h^r\right]^d$.

Let $K^+, K^- \in \mathcal{T}_h$ and $e = \partial K^- \cap \partial K^+$. Choose $x \in e$ such that the vectors $\mathbf{n}_{K^\pm}$ are well defined. Then, for $v \in \mathcal{V}_h$, we define the traces $v_\pm$ by

$$v_\pm(x) = \lim_{\varepsilon \to 0^+} v\left(x - \varepsilon \mathbf{n}_{K^\pm}\right).$$

Without loss of generality we assume that the global labelling number of K^+ is larger than that of K^-. We then define the jumps and averages across the $(d-1)$-dimensional simplex e as

$$[v]_e \equiv v_+ - v_-, \qquad \{v\}_e \equiv \frac{1}{2}\left(v_+ + v_-\right), \qquad \forall\, v \in \mathcal{V}_h.$$

If K^+ is a boundary simplex, then for the boundary $(d-1)$-dimensional simplex $e = \partial K^+ \cap \partial\Omega$, we define $[v]_e \equiv v_+$ and $\{v\}_e \equiv v_+$. Lastly, we set $(n_e^{(1)}, n_e^{(2)}, \cdots, n_e^{(d)})^{\mathrm{T}}$ $\mathbf{n}_e \equiv \mathbf{n}_{K^+}|_e = -\mathbf{n}_{K^-}|_e$ to be the unit normal on e.

Remark 2 The definitions of the jump operator and the global unit normal vector are a bit different from the conventions used in [17, 23], which will lead to slightly different positive and negative signs in the definitions of Sect. 2.3. The choice in this paper leads to more natural positive and negative signs in the analysis of Sect. 4.

Lastly, we introduce a particular way to vectorize a grid function $v_h \in V_h^r$ that will be useful in proving the admissibility of our DWDG schemes. Let N denote the dimension of the space V_h^r, and let $\{\phi_{h,i}\}_{i=1}^N \subset V_h^r$ be an orthonormal basis with respect to the inner product $(\cdot,\cdot)_{\mathcal{T}_h}$. We note that such a basis does exist, but it is introduced purely for the purpose of analyzing the proposed scheme. Then, for any $v_h \in V_h^r$, there exist constants c_k for $k = 1, 2, \cdots, N$ such that $v_h = \sum_{i=1}^N c_k \phi_{h,i}$. Furthermore, there holds

$$\|v_h\|^2_{L^2(\mathcal{T}_h)} = (v_h, v_h)_{\mathcal{T}_h} = \sum_{k=1}^N \sum_{j=1}^N c_k c_j (\phi_{h,k}, \phi_{h,j})_{\mathcal{T}_h} = \sum_{k=1}^N c_k^2 = \|\mathbf{c}\|^2_{\ell^2}$$

for $\mathbf{c} \in \mathbb{R}^N$ with $[\mathbf{c}]_k = c_k$. We call the vector $\mathbf{c}$ the vectorization of v_h and note that we have formed an isometry between the space V_h^r and $\mathbb{R}^N$. Notationally, we will let $\|\cdot\|_{\ell^2,N} = \|\cdot\|_{\ell^2}$ denote the dependence on the number of degrees of freedom defined by the choice $\mathcal{T}_h$ and r when choosing the space V_h^r. Similarly, we use the notation $\|\cdot\|_{L^2(\mathcal{T}_h)}$ to emphasize the triangulation even though we can identify any function in V_h^r with a function in $L^2(\Omega)$ by redefining the discrete function on a set of measure zero corresponding to $\mathcal{E}_h^{\mathbf{I}}$.

2.3 DG Derivative Operators

In this section, we recall the DG derivative operators that were introduced in [17] and will be used later to formulate our DG methods. For the remainder of the section, let $i \in \{1, 2, \cdots, d\}$ and $v \in \mathcal{V}_h$ be fixed.

We first define two trace operators on $e \in \mathcal{E}_h^{\mathrm{I}}$ in the direction x_i:

$$\mathcal{Q}_i^{\pm}(v) \equiv \{v\} \pm \frac{1}{2}\mathrm{sgn}(n_e^{(i)})[v], \quad \text{where} \quad \mathrm{sgn}(n_e^{(i)}) = \begin{cases} 1, & \text{if } n_e^{(i)} > 0, \\ -1, & \text{if } n_e^{(i)} < 0, \\ 0, & \text{if } n_e^{(i)} = 0. \end{cases} \tag{5}$$

The operators $\mathcal{Q}_i^-(v)$ and $\mathcal{Q}_i^+(v)$ can be regarded, respectively, as the "backward" and "forward" limit of v in the x_i direction on $e \in \mathcal{E}_h^{\mathrm{I}}$, where the "forward" and "backward" directions are determined by the choice of the global labelling. On a boundary simplex $e \in \mathcal{E}_h^{\mathrm{B}}$, we simply take $\mathcal{Q}_i^{\pm}(v) = v$.

Using the trace operators, we now define corresponding "backward" and "forward" discrete partial derivative operators $\partial_{h,x_i}^{\pm} : \mathcal{V}_h \to V_r^h$.

Definition 2 Let $v \in \mathcal{V}_h$, $g \in L^1(\partial\Omega)$.

(i) The discrete partial derivatives $\partial_{h,x_i}^{\pm} : \mathcal{V}_h \to V_h^r$ are defined by

$$\left(\partial_{h,x_i}^{\pm} v, w_h\right)_{\mathcal{T}_h} \equiv \left\langle v n^{(i)}, w_h \right\rangle_{\mathcal{E}_h^{\mathrm{B}}} - \left\langle \mathcal{Q}_i^{\pm}(v) n^{(i)}, [w_h] \right\rangle_{\mathcal{E}_h^{\mathrm{I}}} - \left(v, \partial_{x_i} w_h\right)_{\mathcal{T}_h}, \quad \forall w_h \in V_h^r.$$

Here, ∂_{x_i} denotes the usual (weak) partial derivative operator in the direction x_i and $n^{(i)}$ is the piecewise constant vector-valued function satisfying $n^{(i)}|_e = n_e^{(i)}$.

(ii) The discrete partial derivatives with given boundary data $\partial_{h,x_i}^{\pm,g} : \mathcal{V}_h \to V_h^r$ are defined by

$$\left(\partial_{h,x_i}^{\pm,g} v, w_h\right)_{\mathcal{T}_h} \equiv \left(\partial_{h,x_i}^{\pm} v, w_h\right)_{\mathcal{T}_h} + \left\langle (g - v) n^{(i)}, w_h \right\rangle_{\mathcal{E}_h^{\mathrm{B}}}, \qquad \forall w_h \in V_h^r.$$

(iii) The central discrete partial derivatives $\overline{\partial}_{h,x_i}, \overline{\partial}_{h,x_i}^{g} : \mathcal{V}_h \to V_h^r$ are defined by

$$\overline{\partial}_{h,x_i} \equiv \frac{1}{2}\left(\partial_{h,x_i}^{+} + \partial_{h,x_i}^{-}\right), \qquad \overline{\partial}_{h,x_i}^{g} \equiv \frac{1}{2}\left(\partial_{h,x_i}^{+,g} + \partial_{h,x_i}^{+,g}\right).$$

(iv) The discrete gradient operators $\nabla_h^{\pm}, \overline{\nabla}_h, \nabla_{h,g}^{\pm}, \overline{\nabla}_{h,g} : \mathcal{V}_h \to \mathbf{V}_h^r$ are defined as

$$\left(\nabla_h^{\pm} v\right)_i \equiv \partial_{h,x_i}^{\pm} v, \qquad \left(\overline{\nabla}_h v\right)_i \equiv \overline{\partial}_{h,x_i} v,$$
$$\left(\nabla_{h,g}^{\pm} v\right)_i \equiv \partial_{h,x_i}^{\pm,g} v, \qquad \left(\overline{\nabla}_{h,g} v\right)_i \equiv \overline{\partial}_{h,x_i}^{g} v.$$

The above discrete gradient approximations have all been shown in [17] to correspond to the L^2 projection of the gradient of a function v provided $v \in H^1(\Omega)$ and the L^2 projection of the distributional derivative for weaker functions.

2.4 A Skew-Symmetric Derivative Operator

In this section we define a new discrete derivative operator that is skew-symmetric when the boundary data $g = 0$. The derivative operator is key in the definition of our DG methods. Observe that, by [17], we have the following adjoint relationships:

$$\left(\partial^{\pm}_{h,x_i} v_h, w_h\right)_{\mathcal{T}_h} = -\left(v_h, \partial^{\mp,0}_{h,x_i} w_h\right)_{\mathcal{T}_h}, \tag{6a}$$

$$\left(\partial^{\pm,0}_{h,x_i} v_h, w_h\right)_{\mathcal{T}_h} = -\left(v_h, \partial^{\mp}_{h,x_i} w_h\right)_{\mathcal{T}_h} = -\left(v_h, \partial^{\mp,0}_{h,x_i} w_h\right)_{\mathcal{T}_h} - \left\langle v_h, w_h n^{(i)}\right\rangle_{\mathcal{E}_h^{\mathrm{B}}} \tag{6b}$$

for all $v_h, w_h \in V_h^r$. Thus, averaging the two equations, there holds

$$\left(\overline{\partial}_{h,x_i} v_h, w_h\right)_{\mathcal{T}_h} = -\left(v_h, \overline{\partial}^{0}_{h,x_i} w_h\right)_{\mathcal{T}_h}, \tag{7a}$$

$$\left(\overline{\partial}^{0}_{h,x_i} v_h, w_h\right)_{\mathcal{T}_h} = -\left(v_h, \overline{\partial}_{h,x_i} w_h\right)_{\mathcal{T}_h} = -\left(v_h, \overline{\partial}^{0}_{h,x_i} w_h\right)_{\mathcal{T}_h} - \left\langle v_h, w_h n^{(i)}\right\rangle_{\mathcal{E}_h^{\mathrm{B}}} \tag{7b}$$

for all $v_h, w_h \in V_h^r$.

Definition 3 Let $v \in \mathcal{V}_h,\ g \in L^1(\partial\Omega)$. The skewed discrete partial derivative $\widetilde{\partial}^{g}_{h,x} : \mathcal{V}_h \to V_h^r$ is defined by

$$\widetilde{\partial}^{g}_{h,x_i} \equiv \overline{\partial}^{g}_{h,x_i} + \frac{1}{2}\left(\overline{\partial}_{h,x_i} - \overline{\partial}^{g}_{h,x_i}\right) = \frac{1}{2}\overline{\partial}^{g}_{h,x_i} + \frac{1}{2}\overline{\partial}_{h,x_i}. \tag{8}$$

The corresponding skewed discrete gradient operator $\widetilde{\nabla}_{h,g} : \mathcal{V}_h \to \mathbf{V}_h^r$ is defined by $\left(\widetilde{\nabla}_{h,g} v\right)_i \equiv \widetilde{\partial}^{g}_{h,x_i} v$ for all $i = 1, 2, \cdots, d$.

Lemma 1 *The derivative operator $\widetilde{\partial}^{0}_{h,x_i}$ is skew symmetric when the inputs are restricted to be in V_h^r.*

Proof Let $v_h, w_h \in V_h^r$. Observe that

$$\begin{aligned}
\left(\widetilde{\partial}^{0}_{h,x_i} v_h, w_h\right)_{\mathcal{T}_h} &= \left(\overline{\partial}^{0}_{h,x_i} v_h, w_h\right)_{\mathcal{T}_h} + \frac{1}{2}\left(\overline{\partial}_{h,x_i} v_h, w_h\right)_{\mathcal{T}_h} - \frac{1}{2}\left(\overline{\partial}^{0}_{h,x_i} v_h, w_h\right)_{\mathcal{T}_h} \\
&= \left(\overline{\partial}^{0}_{h,x_i} v_h, w_h\right)_{\mathcal{T}_h} + \frac{1}{2}\left\langle v_h, w_h n^{(i)}\right\rangle_{\mathcal{E}_h^{\mathrm{B}}} \\
&= -\left(v_h, \overline{\partial}^{0}_{h,x_i} w_h\right)_{\mathcal{T}_h} - \frac{1}{2}\left\langle v_h, w_h n^{(i)}\right\rangle_{\mathcal{E}_h^{\mathrm{B}}} \\
&= -\left(v_h, \overline{\partial}^{0}_{h,x_i} w_h\right)_{\mathcal{T}_h} - \frac{1}{2}\left(v_h, \overline{\partial}_{h,x_i} w_h\right)_{\mathcal{T}_h} + \frac{1}{2}\left(v_h, \overline{\partial}^{0}_{h,x_i} w_h\right)_{\mathcal{T}_h} \\
&= -\left(v_h, \widetilde{\partial}^{0}_{h,x_i} w_h\right)_{\mathcal{T}_h}.
\end{aligned}$$

The proof is complete.

Remark 3 Skew symmetry breaks down when degrees of freedom are on the boundary of the domain. In finite difference or finite element where the boundary condition is strongly enforced by being built into the approximation space, the partial derivative approximations / difference quotients are skew symmetric after eliminating the degrees of freedom / grid function values on the boundary. In DG, the degrees of freedom cannot directly be associated with boundary data. Instead, the proposed skewed discrete partial derivatives naturally enforce a Dirichlet boundary condition by averaging the gradient that treats the boundary data as fixed and the one where the boundary data is treated as an unknown providing a balance between imposing boundary degrees of freedom versus treating all degrees of freedom as interior.

2.5 DWDG Approximations of the Laplace Operator

In this section we recall the definition of the DWDG approximations of the Laplace operator which were originally introduced in [16, 17, 23] for approximating the Poisson problem. The DWDG approximations $\Delta_h, \Delta_{h,g} : V_h^r \to V_h^r$ of the Laplacian Δ are defined as follows:

$$\Delta_h v_h \equiv -\frac{1}{2}\sum_{i=1}^{d}\left(\partial_{h,x_i}^{+}\partial_{h,x_i}^{-} + \partial_{h,x_i}^{-}\partial_{h,x_i}^{+}\right)v_h, \qquad \forall v_h \in V_h^r, \tag{9a}$$

$$\Delta_{h,g} v_h \equiv -\frac{1}{2}\sum_{i=1}^{d}\left(\partial_{h,x_i}^{+}\partial_{h,x_i}^{-,g} + \partial_{h,x_i}^{-}\partial_{h,x_i}^{+,g}\right)v_h, \qquad \forall v_h \in V_h^r. \tag{9b}$$

Note that the non-mixed one-sided (or one-wind) second order partial derivatives $\partial_{h,x_i}^{+}\partial_{h,x_i}^{+}$ and $\partial_{h,x_i}^{-}\partial_{h,x_i}^{-}$ do not appear in the above discrete Laplace operators. This is the reason why the above discrete operators are called dual-wind DG operators, and it is analogous to alternating between upwind and downwind fluxes as is typical for dynamic problems. The averaging is different than the approach typically used for dynamic problems, and it ensures the discrete operator in (9b) is symmetric when $g = 0$. Multiplying both sides of (9b) by a test function and integrating, there holds

$$\begin{aligned}-\left(\Delta_{h,g} v_h, w_h\right)_{\mathcal{T}_h} = \frac{1}{2}\left(\nabla_{h,0}^{+} v_h, \nabla_{h,0}^{+} w_h\right)_{\mathcal{T}_h} + \frac{1}{2}\left(\nabla_{h,0}^{-} v_h, \nabla_{h,0}^{-} w_h\right)_{\mathcal{T}_h} \\ + \left\langle g, \overline{\nabla}_{h,0} w_h \cdot \mathbf{n}\right\rangle_{\mathcal{E}_h^{\mathrm{B}}}, \qquad \forall w_h \in V_h^r\end{aligned}$$

for all $v_h \in V_h^r$. We note that the operator $\Delta_{h,g}$ defined in (9b) is the one considered in [23] for the Dirichlet problem. The method was extended to Neumann problems in [16]. In one dimension, the corresponding discrete Laplacian operator in [16] would correspond to the combination $\frac{1}{2}\partial_{h,x}^{+,g}\partial_{h,x} + \frac{1}{2}\partial_{h,x_i}^{-,g}\partial_{h,x_i}^{+}$, where it is assumed $u_x(b) = g(b)$ and $-u_x(a) = g(a)$ for $\Omega = (a, b)$. Thus, we see the DWDG method allows for a natural enforcement of boundary conditions depending on if the boundary condition should act on u or $\nabla u \cdot \mathbf{n}$.

3 Formulations of Dual-Wind DG Methods for Problems (1) and (2)

In this section we introduce a class of DWDG methods for approximating both (1) and (2) in a unified fashion. Since $\mathcal{H}$ is nonlinear in (2) and (1), it is not possible to multiply by a test function and apply integration by parts. Instead, we project the nonlinearity directly into the discrete space. We also directly approximate ∇u with an appropriate DG derivative operator. Lastly, we introduce standard jump/penalization terms. Consequently, we discretize (2) by seeking a solution $u_h \in V_h^r$ such that

$$\begin{aligned}
&\frac{\sigma_h}{2}\left(\nabla_{h,0}^{+}u_h, \nabla_{h,0}^{+}w_h\right)_{\mathcal{T}_h} + \frac{\sigma_h}{2}\left(\nabla_{h,0}^{-}u_h, \nabla_{h,0}^{-}w_h\right)_{\mathcal{T}_h} + \theta_h\left(u_h, w_h\right)_{\mathcal{T}_h} \\
&+ \left(\mathcal{H}(\widetilde{\nabla}_{h,g}u_h, u_h, \cdot), w_h\right)_{\mathcal{T}_h} + \left\langle \frac{\gamma_e}{h_e}[u_h], [w_h]\right\rangle_{\mathcal{E}_h} \\
&= -\sigma_h\left\langle g, \overline{\nabla}_{h,0}w_h \cdot \mathbf{n}\right\rangle_{\mathcal{E}_h^{\mathrm{B}}} + \left\langle \frac{\gamma_e}{h_e}g, w_h\right\rangle_{\mathcal{E}_h^{\mathrm{B}}}
\end{aligned} \tag{10}$$

for all $w_h \in V_h^r$, where $\gamma_e \geqslant 0$ is a penalty parameter defined on $e \in \mathcal{E}_h$ and $\sigma_h \to \sigma$ and $\theta_h \to \theta$ as $h \to 0^+$.

Define the stabilization operator $J_{h,g} : \mathcal{V}_h \to V_h^r$ by

$$\left(J_{h,g}(v), w_h\right)_{\mathcal{T}_h} = \sum_{e\in\mathcal{E}_h^{\mathrm{I}}}\left\langle \frac{\gamma_e}{h_e}[v], [w_h]\right\rangle_e + \sum_{e\in\mathcal{E}_h^{\mathrm{B}}}\left\langle \frac{\gamma_e}{h_e}(v-g), w_h\right\rangle_e, \qquad \forall\, w_h \in V_h^r, \tag{11}$$

and let $\mathbb{P}_h^r : L^2(\Omega) \to V_h^r$ denote the L^2 projection operator into V_h^r that satisfies

$$\left(\mathbb{P}_h^r v, w_h\right)_{\mathcal{T}_h} = \left(v, w_h\right)_{\mathcal{T}_h}, \qquad \forall\, w_h \in V_h^r. \tag{12}$$

Then, the weak form (10) can be written compactly as seeking a solution $u_h \in V_h^r$ such that

$$0 = \mathcal{H}_h^{\sigma}[u_h] \equiv -\sigma_h\Delta_{h,g}u_h + \mathbb{P}_h^r\mathcal{H}(\widetilde{\nabla}_{h,g}u_h, u_h, x) + \theta_h u_h + J_{h,g}(u_h). \tag{13}$$

Similarly, we discretize (1) by seeking a solution $u_h \in V_h^r$ such that

$$0 = \mathcal{H}_h[u_h] \equiv -\sigma_h\Delta_{h,g}u_h + \mathbb{P}_h^r\mathcal{H}(\widetilde{\nabla}_{h,g}u_h, u_h, x) + \theta_h u_h + J_{h,g}(u_h), \tag{14}$$

where $\sigma_h \geqslant 0$ and $-\sigma_h\Delta_{h,g}$ is an optional vanishing viscosity stabilization term. In practice, $\sigma_h \to 0^+$ and $\theta_h \to \theta$ as $h \to 0^+$. In Sect. 4 we shall see that $\sigma_h = \gamma_e = 0$ still admits a unique solution u_h to (14) as long as $\max\{\kappa_0, \theta_h\} > 0$. We also see that if we further assume $\sigma_h > 0$ and $\max\{\kappa_0, \theta\} > 0$, then the unique solution is L^2 stable independent of the magnitude of σ_h.

In the remainder of this paper we shall focus on scheme (14) for approximating (1) because scheme (10) is contained in (14) as a special case with the natural choice $\sigma_h = \sigma + \mathcal{O}(h^p)$ for various powers $p > 0$. In the numerical tests of Sect. 5 we shall consider the choice $\sigma_h = \sigma + h^p$ with $\sigma > 0$ if we are approximating (2) and $\sigma = 0$ if we are approximating (1). In addition, we shall also consider the case $\theta = \theta_h \in \mathcal{O}(h^p)$ to see how well (14) can approximate (1) in the degenerate limiting case $\theta = 0$.

Remark 4

(a) When $\sigma_h > 0$, the above methods are dual-wind methods because the discrete Laplace operator $\Delta_{h,g}$ is used to approximate the Laplace operator Δ. The resulting stabilization term is naturally motivated by the vanishing viscosity approach to define viscosity solutions of (1). The skewed discrete gradient operator $\widetilde{\nabla}_{h,g}$ also utilizes both upwind and downwind fluxes.

(b) We note that the admissibility and stability results in this paper hold for any choice $\sigma_h > 0$. In contrast to monotone methods, we are not limited to the choice $\sigma_h \in \mathcal{O}(h)$ in (14) when approximating (1). Indeed, we uniformly observe optimal L^2 rates in Sect. 5 when choosing piecewise linear basis functions with $\sigma_h = \sigma + h^2$ and $\theta_h = \theta + h^2$. In some nonlinear tests, we also observe higher rates of convergence when choosing higher degree basis functions and higher order scalings for σ_h and θ_h. We are also able to achieve optimal rates for higher degree basis functions for a linear benchmark problem that is convection-dominated with meshes that do not resolve the small diffusion parameter.

4 Admissibility and Stability Analysis

In this section, we show that the DG scheme defined by (14) has a unique solution for all $\theta_h > 0$ even in the degenerate case when $\theta = 0$. Furthermore, we also prove an L^2 stability estimate for the numerical solution under the condition $\max\{\kappa_0, \theta\} > 0$ and $\sigma_h > 0$.

To motivate the proof, first assume that $\mathcal{H}$ is linear and can be written as $(AD + kI)\mathbf{c} = \mathbf{F}$ for $\mathbf{c}$ the coefficients of the unknown function $u_h \in V_h^r$, A symmetric positive definite, D antisymmetric, and $k > 0$. Then, there exists a non-singular matrix R such that $A = R^{\mathrm{T}}R$ is a Choleski factorization of A, and we have

$$AD + kI = R^{\mathrm{T}}\left(RDR^{\mathrm{T}} + kI\right)(R^{\mathrm{T}})^{-1}.$$

Thus, $AD + kI$ is similar to $RDR^{\mathrm{T}} + kI$. Since RDR^{T} is antisymmetric, all of its eigenvalues are purely imaginary. Hence, all eigenvalues of $RDR^{\mathrm{T}} + kI$ have the real component k, and it follows that $AD + kI$ must be non-singular. In the proof, we account for the facts that A may not be symmetric positive definite and each partial derivative contributes an antisymmetric matrix corresponding to $\widetilde{\partial}^0_{h,x_i}$. We also linearize $\mathcal{H}$ via the mean value theorem and its Lipschitz continuity. Lastly, we use the observation that

$$\begin{aligned}\left(RDR^{\mathrm{T}} + kI\right)^{\mathrm{T}}\left(RDR^{\mathrm{T}} + kI\right) &= -RDADR^{\mathrm{T}} - kRDR^{\mathrm{T}} + kRDR^{\mathrm{T}} + k^2 I \\ &= -RDADR^{\mathrm{T}} + k^2 I\end{aligned}$$

allowing a way to uniformly bound all of the singular values of $AD + kI$. The skew-symmetry is key for eliminating the cross-term that would be proportional to k instead of k^2. In the proof, we will use the convention that for any symmetric matrices B and C, $B \leqslant C$ if $C - B$ is nonnegative definite.

The admissibility and stability analysis exploit properties of the mapping $\mathcal{M}_\rho : V_h^r \to V_h^r$ defined by $\widehat{v}_h = \mathcal{M}_\rho v_h$ where

$$\widehat{v}_h = \mathcal{M}_\rho v_h = v_h - \rho\mathcal{H}_h[v_h] \tag{15}$$

for some constant $\rho > 0$. Clearly a fixed point of $\mathcal{M}_\rho$ is a solution to (14). Below we show $\mathcal{M}_\rho$ is a contraction with respect to the L^2 norm for sufficiently small $\rho > 0$ from which the existence and uniqueness of solutions to (14) follow readily by the contractive mapping theorem (cf. [30]).

Lemma 2 *Suppose the operator $\mathcal{H}$ in* (1) *or* (2) *is Lipschitz continuous with respect to its first two arguments and nondecreasing with respect to its second argument. For any $u_h, v_h \in V_h^r$, let $\widehat{u}_h = \mathcal{M}_\rho u_h$ and $\widehat{v}_h = \mathcal{M}_\rho v_h$. Then there exists a constant $\rho_0 > 0$ such that for all $0 < \rho < \rho_0$ there holds*

$$\|\widehat{u}_h - \widehat{v}_h\|_{L^2(\mathcal{T}_h)} \leqslant \left(1 - \frac{\rho(\sigma_h \lambda + \theta_h + \kappa_0)}{2}\right) \|u_h - v_h\|_{L^2(\mathcal{T}_h)}$$

provided $\min\{\kappa_0, \sigma_h, \theta_h\} \geqslant 0$ *and* $\max\{\kappa_0, \sigma_h, \theta_h\} > 0$. *Notationally, λ is a positive lower bound for the minimal eigenvalue of the operator $-\Delta_{h,0}$.*

Proof Define $w_h = u_h - v_h$ and $\widehat{w}_h = \widehat{u}_h - \widehat{v}_h$. Then, there holds

$$\begin{aligned}
\widehat{w}_h &= \widehat{u}_h - \widehat{v}_h = \mathcal{M}_\rho u_h - \mathcal{M}_\rho v_h \\
&= w_h + \rho\sigma_h \Delta_{h,0} w_h - \rho\theta_h w_h - \rho J_{h,0}(w_h) \\
&\quad - \rho\left(\mathbb{P}_h^r\Big(\mathcal{H}(\widetilde{\nabla}_{h,g} u_h, u_h, x)\Big) - \mathbb{P}_h^r\Big(\mathcal{H}(\widetilde{\nabla}_{h,g} v_h, v_h, x)\Big)\right).
\end{aligned} \tag{16}$$

We seek to apply the mean value theorem to simplify the nonlinear terms in (16). Since $\mathcal{H}$ is not necessarily differentiable with respect to its first two arguments, where the first argument has d components, we cannot apply the classical mean value theorem. However, by the Lipschitz continuity assumption for $\mathcal{H}$, we do have $\mathcal{H}$ is differentiable almost everywhere in $\mathbb{R}^d \times \mathbb{R}$ by Rademacher's theorem. Thus, we can apply a generalized version of the mean value theorem to find functions $\mathcal{H}_i : \Omega \to \mathbb{R}$ for $i = 0, 1, \cdots, d$ such that

$$\mathcal{H}(\widetilde{\nabla}_{h,g} u_h, u_h, \cdot) - \mathcal{H}(\widetilde{\nabla}_{h,g} v_h, v_h, \cdot) = \mathcal{H}_0(\cdot)(u_h - v_h) + \sum_{i=1}^{d} \mathcal{H}_i(\cdot)\Big(\widetilde{\partial}_{h,x_i}^g u_h - \widetilde{\partial}_{h,x_i}^g v_h\Big),$$

where

$$\mathcal{H}_0(x) = \int_0^1 \partial_{d+1}\mathcal{H}\Big(t\widetilde{\nabla}_{h,g} u_h + (1-t)\widetilde{\nabla}_{h,g} v_h, tu_h + (1-t)v_h, x\Big)\mathrm{d}t$$

and

$$\mathcal{H}_i(x) = \int_0^1 \partial_i \mathcal{H}\Big(t\widetilde{\nabla}_{h,g} u_h + (1-t)\widetilde{\nabla}_{h,g} v_h, tu_h + (1-t)v_h, x\Big)\mathrm{d}t$$

for all $i = 1, 2, \cdots, d+1$. Here, the partial derivatives of the Hamiltonian with respect to the i-th argument $\partial_i H$ for $i = 1, 2, \cdots, d+1$ are defined almost everywhere by the Lipschitz continuity of $\mathcal{H}$. By the definition of $\mathbb{P}_h^r$, the last term in (16) can be linearized in its weak form by observing that

$$\begin{aligned}
&\Big(\mathcal{H}(\widetilde{\nabla}_{h,g}u_h,u_h,\cdot),\phi_h\Big)_{\mathcal{T}_h}-\Big(\mathcal{H}(\widetilde{\nabla}_{h,g}v_h,v_h,\cdot),\phi_h\Big)_{\mathcal{T}_h}\\
&=\sum_{i=1}^{d}\Big(\mathcal{H}_i(\widetilde{\partial}^g_{h,x_i}u_h-\widetilde{\partial}^g_{h,x_i}v_h),\phi_h\Big)_{\mathcal{T}_h}+\big(\mathcal{H}_0(u_h-v_h),\phi_h\big)_{\mathcal{T}_h}\\
&=\sum_{i=1}^{d}\Big(\mathcal{H}_i\widetilde{\partial}^0_{h,x_i}w_h,\phi_h\Big)_{\mathcal{T}_h}+\big(\mathcal{H}_0w_h,\phi_h\big)_{\mathcal{T}_h}
\end{aligned}$$

for all $\phi_h\in V_h^r$. Let $\mathbf{e}_i\in\mathbb{R}^d$ denote the i-th Canonical basis vector of $\mathbb{R}^d$. Then, by (3), there holds

$$\sup_{\tau\to0}\frac{\big|\mathcal{H}(\mathbf{z}+\tau\mathbf{e}_i,z,x)-\mathcal{H}(\mathbf{z},z,x)\big|}{|\tau|}\leqslant\kappa,\qquad\sup_{\tau\to0}\frac{|\mathcal{H}(\mathbf{z},z+\tau,x)-\mathcal{H}(\mathbf{z},z,x)|}{|\tau|}\leqslant\kappa$$

for all $x\in\Omega$. Hence, $\sup_{x\in\Omega}|\mathcal{H}_i|\leqslant\kappa$ for all $i=0,1,\cdots,d$. Similarly, $\inf_{x\in\Omega}\mathcal{H}_0\geqslant\kappa_0$ by (4). Define the positive functions $\mathcal{H}_i^{\pm}$ such that

$$\mathcal{H}_i^+\equiv1+\max\big\{\mathcal{H}^i,0\big\},\qquad\mathcal{H}_i^-\equiv1-\min\big\{\mathcal{H}^i,0\big\}$$

so that $\mathcal{H}^i=\mathcal{H}_i^+-\mathcal{H}_i^-$ with $1\leqslant\mathcal{H}_i^{\pm}\leqslant1+\kappa$. Plugging this into (16), there holds

$$\begin{aligned}
\widehat{w}_h=&\,w_h+\rho\sigma_h\Delta_{h,0}w_h-\rho\theta_hw_h-\rho J_{h,0}(w_h)\\
&-\rho\sum_{i=1}^{d}\mathbb{P}_h^r\Big(\mathcal{H}_i^+\widetilde{\partial}^0_{h,x_i}w_h\Big)+\rho\sum_{i=1}^{d}\mathbb{P}_h^r\Big(\mathcal{H}_i^-\widetilde{\partial}^0_{h,x_i}w_h\Big)-\rho\mathbb{P}_h^r\big(\mathcal{H}_0w_h\big).
\end{aligned}\tag{17}$$

Consider the basis $\{\phi_{h,i}\}_{i=1}^N\subset V_h^r$ introduced in Sect. 2.2. Then, the associated mass matrix is the identity matrix I. Also let L denote the matrix representation of $-\Delta_{h,0}$, J denote the corresponding matrix representation of $J_{h,0}$, and D_i denote the corresponding matrix representation of $\widetilde{\partial}^0_{h,x_i}$. Then, L is symmetric positive definite; J is symmetric nonnegative definite; and D_i is skew-symmetric. Since $0\leqslant\kappa_0\leqslant\mathcal{H}_0\leqslant\kappa$, the matrix A_0 defined by $[A_0]_{ij}\equiv\big(\mathcal{H}_0\phi_{h,i},\phi_{h,j}\big)_{\mathcal{T}_h}$ is symmetric nonnegative definite with $\kappa_0I\leqslant A_0\leqslant\kappa I$. Indeed, for any function $z_h\in V_h^r$ with a vectorization $\mathbf{z}\in\mathbb{R}^N$, there holds

$$\begin{aligned}
\mathbf{z}^{\mathrm{T}}A_0\mathbf{z}=&\sum_{i=1}^{N}\sum_{j=1}^{N}z_iz_j\big(\mathcal{H}_0\phi_{h,i},\phi_{h,j}\big)_{\mathcal{T}_h}=\sum_{i=1}^{N}z_i\Big(\mathcal{H}_0\phi_{h,i},\sum_{j=1}^{N}z_j\phi_{h,j}\Big)_{\mathcal{T}_h}\\
=&\Big(\mathcal{H}_0\sum_{i=1}^{N}z_i\phi_{h,i},\sum_{j=1}^{N}z_j\phi_{h,j}\Big)_{\mathcal{T}_h}=\big(\mathcal{H}_0z_h,z_h\big)_{\mathcal{T}_h}=\int_{\Omega}\mathcal{H}_0z_h^2\mathrm{d}x\\
=&\,\overline{\kappa}\big(z_h,z_h\big)_{\mathcal{T}_h}=\overline{\kappa}\|z_h\|^2_{L^2(\mathcal{T}_h)}=\overline{\kappa}\|\mathbf{z}\|^2_{\ell^2,N}
\end{aligned}$$

for some $\overline{\kappa}\in[\kappa_0,\kappa]$ by the integral mean value theorem. Thus, all eigenvalues of the symmetric matrix A_0 are in the interval $[\kappa_0,\kappa]$ by way of the Rayleigh Quotient. Similarly, the matrices $A_i^{\pm}$ defined by $[A_i^{\pm}]_{kj}\equiv\big(\mathcal{H}_i^{\pm}\phi_{h,k},\phi_{h,j}\big)_{\mathcal{T}_h}$ are symmetric positive definite with $I\leqslant A_i^{\pm}\leqslant(1+\kappa)I$.

Let $\mathbf{w},\widehat{\mathbf{w}}\in\mathbb{R}^N$ denote the coefficients for w_h and $\widehat{w}_h$, respectively. Multiplying (17) by $\phi_{h,j}$ for each $j\in\{1,2,\cdots,N\}$ and integrating over Ω, there holds

$$\begin{aligned}\widehat{\mathbf{w}} &= \mathbf{w} - \rho\sigma_h L\mathbf{w} - \rho\theta_h \mathbf{w} - \rho J\mathbf{w} - \rho A_0\mathbf{w} - \rho\sum_{i=1}^{d} A_i^+ D_i\mathbf{w} + \rho\sum_{i=1}^{d} A_i^- D_i\mathbf{w}\\ &= \Big(I - \rho\sigma_h L - \rho\theta_h I - \rho J - \rho A_0 - \rho\sum_{i=1}^{d} A_i^+ D_i + \rho\sum_{i=1}^{d} A_i^- D_i\Big)\mathbf{w}\\ &\equiv A\mathbf{w}.\end{aligned}$$

Hence, it suffices to show that

$$\|A\mathbf{w}\|_{\ell^2,N} \leqslant \Big(1 - \frac{\rho c}{2}\Big)\|\mathbf{w}\|_{\ell^2,N} \tag{18}$$

for all $\rho > 0$ sufficiently small and some $c > 0$. To that end, let $\lambda > 0$ denote the minimum eigenvalue of L. Then, there exists a constant $R_1 > 0$ such that

$$\frac{1}{2}I - \rho\sigma_h L - \rho\theta_h I - \rho A_0 - \rho J \geqslant 0 \tag{19}$$

for all $\rho \leqslant R_1$. Thus,

$$\begin{aligned}\|A\mathbf{w}\|_{\ell^2,N} &\leqslant \Big\|\Big(\frac{1}{2}I - \rho\sigma_h L - \rho\theta_h I - \rho A_0 - \rho J\Big)\mathbf{w}\Big\|_{\ell^2,N}\\ &\quad + \sum_{i=1}^{d}\Big\|\Big(\frac{1}{4d}I - \rho A_i^+ D_i\Big)\mathbf{w}\Big\|_{\ell^2,N} + \sum_{i=1}^{d}\Big\|\Big(\frac{1}{4d}I + \rho A_i^- D_i\Big)\mathbf{w}\Big\|_{\ell^2,N}\\ &\leqslant \Big(\frac{1}{2} - \rho\sigma_h\lambda - \rho\theta_h - \rho\kappa_0\Big)\|\mathbf{w}\|_{\ell^2,N} + \sum_{i=1}^{d}\Big\|\Big(\frac{1}{4d}I - \rho A_i^+ D_i\Big)\mathbf{w}\Big\|_{\ell^2,N}\\ &\quad + \sum_{i=1}^{d}\Big\|\Big(\frac{1}{4d}I + \rho A_i^- D_i\Big)\mathbf{w}\Big\|_{\ell^2,N}\\ &= \Big(\frac{1}{2} - \rho c\Big)\|\mathbf{w}\|_{\ell^2,N} + \sum_{i=1}^{d}\Big\|\Big(\frac{1}{4d}I - \rho A_i^+ D_i\Big)\mathbf{w}\Big\|_{\ell^2,N}\\ &\quad + \sum_{i=1}^{d}\Big\|\Big(\frac{1}{4d}I + \rho A_i^- D_i\Big)\mathbf{w}\Big\|_{\ell^2,N}\end{aligned} \tag{20}$$

since I, L, A_0, and J are all symmetric nonnegative definite with $A_0 \geqslant \kappa_0 I$, where $c \equiv \sigma_h\lambda + \theta_h + \kappa_0$.

To estimate the last two terms above, define $\lambda_* \equiv \max\{\lambda_j \mid \lambda_j \text{ is an eigenvalue of } -D_j^2 = D_j^{\mathrm{T}} D_j \geqslant 0$ for all $j = 1, 2, \cdots, d\}$. Observe that

$$
\begin{aligned}
&\left\|\left(\frac{1}{8d(\kappa+1)}I \mp \rho D_i\right)\mathbf{w}\right\|^2_{\ell^2,N}\\
&=\mathbf{w}^{\mathrm{T}}\left(\frac{1}{8d(\kappa+1)}I \mp \rho D_i\right)^{\mathrm{T}}\left(\frac{1}{8d(\kappa+1)}I \mp \rho D_i\right)\mathbf{w}\\
&=\mathbf{w}^{\mathrm{T}}\left(\frac{1}{8d(\kappa+1)}I \pm \rho D_i\right)\left(\frac{1}{8d(\kappa+1)}I \mp \rho D_i\right)\mathbf{w}\\
&=\mathbf{w}^{\mathrm{T}}\left(\frac{1}{64d^2(\kappa+1)^2}I \mp \rho\frac{1}{8d(\kappa+1)}D_i \pm \rho\frac{1}{8d(\kappa+1)}D_i - \rho^2 D_i^2\right)\mathbf{w}\\
&=\mathbf{w}^{\mathrm{T}}\left(\frac{1}{64d^2(\kappa+1)^2}I - \rho^2 D_i^2\right)\mathbf{w}\\
&\leqslant\left(\frac{1}{64d^2(\kappa+1)^2} + \rho^2\lambda_*\right)\|\mathbf{w}\|^2_{\ell^2,N}.
\end{aligned}
\tag{21}
$$

Thus,

$$
\begin{aligned}
&\left\|\left(\frac{1}{4d}I \mp \rho A_i^{\pm} D_i\right)\mathbf{w}\right\|_{\ell^2,N}\\
&=\left\|\left(\frac{1}{4d}I - \frac{1}{8d(\kappa+1)}A_i^{\pm} + \frac{1}{8d(\kappa+1)}A_i^{\pm} \mp \rho A_i^{\pm} D_i\right)\mathbf{w}\right\|_{\ell^2,N}\\
&=\left\|\left[\frac{1}{4d}I - \frac{1}{8d(\kappa+1)}A_i^{\pm} + A_i^{\pm}\left(\frac{1}{8d(\kappa+1)}I \mp \rho D_i\right)\right]\mathbf{w}\right\|_{\ell^2,N}\\
&\leqslant\left\|\left(\frac{1}{4d}I - \frac{1}{8d(\kappa+1)}A_i^{\pm} + \sqrt{\frac{1}{64d^2(\kappa+1)^2} + \rho^2\lambda_*}A_i^{\pm}\right)\mathbf{w}\right\|_{\ell^2,N}\\
&=\left\|\left[\frac{1}{4d}I + \left(\sqrt{\frac{1}{64d^2(\kappa+1)^2} + \rho^2\lambda_*} - \frac{1}{8d(\kappa+1)}\right)A_i^{\pm}\right]\mathbf{w}\right\|_{\ell^2,N}\\
&\leqslant\left\|\left[\frac{1}{4d}I + \left(\sqrt{\frac{1}{64d^2} + \rho^2\lambda_*(\kappa+1)^2} - \frac{1}{8d}\right)I\right]\mathbf{w}\right\|_{\ell^2,N}\\
&=\left(\frac{1}{4d} + \sqrt{\frac{1}{64d^2} + \rho^2\lambda_*(\kappa+1)^2} - \frac{1}{8d}\right)\|\mathbf{w}\|_{\ell^2,N}\\
&=\left(\frac{1}{8d} + \sqrt{\frac{1}{64d^2} + \rho^2\lambda_*(\kappa+1)^2}\right)\|\mathbf{w}\|_{\ell^2,N}.
\end{aligned}
$$

Suppose $R_2 > 0$ is defined by

$$
R_2 \equiv \frac{4c}{64d^2\lambda_*(\kappa+1)^2 - 4c^2} = \mathcal{O}(h^2) \tag{22}
$$

since $\lambda_* \in \mathcal{O}(h^{-2})$. Then,

$$
\begin{aligned}
\rho \leqslant R_2 \;&\Longrightarrow\; \rho \leqslant \frac{4c}{64d^2\lambda_*(\kappa+1)^2 - 4c^2} \\
&\Longrightarrow\; \rho\big(64d^2\lambda_*(\kappa+1)^2 - 4c^2\big) - 4c \leqslant 0 \\
&\Longrightarrow\; \rho\big[\rho\big(64d^2\lambda_*(\kappa+1)^2 - 4c^2\big) - 4c\big] \leqslant 0 \\
&\Longrightarrow\; \rho^2 64d^2\lambda_*(\kappa+1)^2 \leqslant \rho 4c + \rho^2 4c^2 \\
&\Longrightarrow\; \frac{1}{64d^2} + \rho^2\lambda_*(\kappa+1)^2 \leqslant \frac{1}{64d^2} + \rho\frac{c}{16d^2} + \rho^2\frac{c^2}{16d^2} \\
&\Longrightarrow\; \sqrt{\frac{1}{64d^2} + \rho^2\lambda_*(\kappa+1)^2} \leqslant \frac{1}{8d} + \rho\frac{c}{4d} \\
&\Longrightarrow\; \frac{1}{8d} + \sqrt{\frac{1}{64d^2} + \rho^2\lambda_i * (\kappa+1)^2} \leqslant \frac{1}{4d} + \rho\frac{c}{4d},
\end{aligned}
$$

and it follows that

$$
\left\|\Big(\frac{1}{4d}I \mp \rho A_i^{\pm} D_i\Big)\mathbf{w}\right\|_{\ell^2,N} \leqslant \Big(\frac{1}{4d} + \rho\frac{c}{4d}\Big)\|\mathbf{w}\|_{\ell^2,N}
$$

for all $i = 1, 2, \cdots, d$. Plugging this into (20), we get

$$
\begin{aligned}
\|\widehat{\mathbf{w}}\|_{\ell^2,N} &= \|A\mathbf{w}\|_{\ell^2,N} \\
&\leqslant \Big(\frac{1}{2} - \rho c\Big)\|\mathbf{w}\|_{\ell^2,N} \\
&\quad + \sum_{i=1}^{d}\left\|\Big(\frac{1}{4d}I - \rho A_i^{+} D_i\Big)\mathbf{w}\right\|_{\ell^2,N} + \sum_{i=1}^{d}\left\|\Big(\frac{1}{4d}I + \rho A_i^{-} D_i\Big)\mathbf{w}\right\|_{\ell^2,N} \\
&\leqslant \Big(\frac{1}{2} - \rho c\Big)\|\mathbf{w}\|_{\ell^2,N} + 2\sum_{i=1}^{d}\Big(\frac{1}{4d} + \rho\frac{c}{4d}\Big)\|\mathbf{w}\|_{\ell^2,N} \\
&= \Big(\frac{1}{2} - \rho c + \frac{1}{2} + \rho\frac{c}{2}\Big)\|\mathbf{w}\|_{\ell^2,N} \\
&= \Big(1 - \rho\frac{c}{2}\Big)\|\mathbf{w}\|_{\ell^2,N}
\end{aligned}
$$

for $c = \sigma_h\lambda + \theta_h + \kappa_0$ and all $0 < \rho < \min\{R_1, R_2\}$, where R_1 is defined by (19) and R_2 is defined by (22). Consequently, $\|\widehat{w}_h\|_{L^2(\mathcal{T}_h)} \leqslant \Big(1 - \rho\frac{c}{2}\Big)\|w_h\|_{L^2(\mathcal{T}_h)}$ for all $\rho > 0$ sufficiently small by the isometry between V_h^r and $\mathbb{R}^N$. The proof is complete.

As an immediate corollary, we have the following admissibility result for the proposed scheme (14).

Theorem 1 *Under the assumptions of Lemma 2, the scheme (14) has a unique solution.*

Proof We have the space $\big(V_h^r, \|\cdot\|_{L^2(\mathcal{T}_h)}\big)$ is a Banach space since it is a finite-dimensional normed vector space. Furthermore, by Lemma 2, there exists a constant $\rho > 0$ for which the operator $\mathcal{M}_\rho : V_h^r \to V_h^r$ is a contraction in $L^2(\mathcal{T}_h)$. By the contractive mapping theorem (cf. [30]), it follows that $\mathcal{M}_\rho$ has a unique fixed point $u_h \in V_h^r$. Thus, there exists a unique solution to the scheme (14) in the space V_h^r since it would follow that $\rho\mathcal{H}_h[u_h] = 0$.

Remark 5

(a) The iteration defined by the mapping $\mathcal{M}_\rho$ can theoretically be used as a global solver for (14) when choosing ρ sufficiently small. By (19) and (22), we have $\rho \in \mathcal{O}(h^2)$.
(b) The above result holds independent of the magnitude of θ_h and σ_h. Thus, we can design a scheme for (1) that formally has optimal order by choosing $\sigma_h \in \mathcal{O}(h^{r+1})$. For degenerate problems with $\kappa_0 = \theta = 0$, we can also formally choose $\theta_h \in \mathcal{O}(h^{r+1})$ with $\theta_h > 0$.

We end this section by deriving an L^2 stability estimate for the numerical solution u_h that solves (10) (equivalently (13)). For $g \neq 0$, the proof is complicated by the fact that mappings $\widetilde{\partial}^g_{h,x_i}, J_{h,g} : \mathcal{V}_h \to V_h^r$ are affine transformations, not linear transformations, due to the source terms associated with the fixed boundary condition. Let 0_h denote the zero function in V_h^r. Observe that, by replacing v with 0 in (11), there holds $(J_{h,g}0_h, w_h)_{\mathcal{T}_h} = -\langle g, w_h\rangle_{\mathcal{E}_h^B}$ for all $w_h \in V_h^r$ due to the fact that $J_{h,g}$ is not a linear transformation for $g \neq 0$. To account for the fact $J_{h,g}$ is not linear when $g \neq 0$, we choose a discrete function $v_h \in V_h^r$ that naturally incorporates the boundary data g in a way that is comparable to how the boundary data affects u_h (see (23) below). We then mod out the boundary condition when $g \neq 0$ by bounding the function $u_h - v_h$. Indeed, by directly comparing u_h to v_h, we have $J_{h,g}u_h - J_{h,g}v_h = J_{h,0}(u_h - v_h)$, where we can now exploit the fact that $J_{h,0}$ is a linear transformation.

Theorem 2 *Suppose the assumptions of Lemma 2 hold. Let u_h be the unique solution to (14) with $\sigma_h > 0$ and $\max\{\kappa_0, \theta\} > 0$. Then there exists a positive constant $C > 0$ independent of h such that*

$$\|u_h\|_{L^2(\mathcal{T}_h)} \leqslant \frac{C}{\kappa_0 + \sigma_h\lambda + \theta}$$

provided $\gamma_e > 0$ for all $e \in \mathcal{E}_h$ in the definition of $J_{h,g}$ or, if $\gamma_e = 0$, then the mesh is quasi-uniform with each boundary simplex having at most one face/edge in $\partial\Omega$.

Proof Let $v_h \in V_h^r$ be the DWDG approximation to v, where the two functions are the unique solutions to

$$0 = -\Delta_{h,g}v_h + \frac{1}{\sigma_h}J_{h,g}(v_h) \tag{23}$$

and

$$\begin{aligned} -\Delta v &= 0 && \text{in } \Omega, \\ v &= g && \text{on } \partial\Omega, \end{aligned}$$

respectively. Then, by [23], there holds $\|v_h - v\|_{L^2(\mathcal{T}_h)} \to 0$, $\|\nabla_{h,g}^{\pm}v_h - \nabla v\|_{L^2(\mathcal{T}_h)} \to 0$, and $\|\nabla_h^{\pm}v_h - \nabla v\|_{L^2(\mathcal{T}_h)} \to 0$. Thus, there exists a constant C_1 independent of h and σ_h depending on $\|v\|_{H^2(\Omega)}$ such that $\|v_h\|_{L^2(\mathcal{T}_h)}$, $\|\nabla_{h,g}^{\pm}v_h\|_{L^2(\mathcal{T}_h)}$, and $\|\nabla_h^{\pm}v_h\|_{L^2(\mathcal{T}_h)}$ are uniformly bounded by C_1. Note that the result holds uniformly for all $\sigma_h > 0$ since $\sigma_h \to 0^+$ implies $v_h \in C^0(\Omega) \cap V_h^r$. To see this, multiply (23) by v_h, integrate, and use the properties of the DWDG method for Poisson's equation and the definition of $J_{h,g}$. We note that the restriction $\gamma_e > 0$ or the mesh is quasi-uniform with boundary simplices having at most one face/edge in $\partial\Omega$ is due to the restrictions assumed in [23].

By the mean value theorem, there exists linear operators $\mathcal{H}_i$ for $i = 0, 1, \cdots, d$ such that

$$\mathcal{H}_h[u_h] - \mathcal{H}_h[v_h] = \sum_{i=0}^{d} \mathcal{H}_i(u_h - v_h).$$

Define $\widetilde{\mathcal{H}}_h[w_h] = \sum_{i=0}^{d} \mathcal{H}_i w_h + \mathcal{H}_h[v_h]$. Then, by Theorem 1, $u_h - v_h$ is the unique solution to the (linear) scheme $\widetilde{\mathcal{H}}_h[w_h] = 0$.

Define $c \equiv \max\{\kappa_0, \sigma_h\lambda, \theta_h\} > 0$. Let $\widetilde{\mathcal{M}}_\rho$ denote the mapping $\mathcal{M}_\rho$ with $\mathcal{H}_h$ replaced by $\widetilde{\mathcal{H}}_h$ in (15). Choose $\rho > 0$ such that the mapping $\widetilde{\mathcal{M}}_\rho$ is a contraction satisfying Lemma 2 so that it has the unique fixed point $u_h - v_h$. Let $\widehat{0}_h = \widetilde{\mathcal{M}}_\rho 0_h$, where $0_h \in V_h^r$ denotes the zero function. Then, there holds

$$\begin{aligned}
\|u_h - v_h\|_{L^2(\mathcal{T}_h)} &= \|\widetilde{\mathcal{M}}_\rho(u_h - v_h)\|_{L^2(\mathcal{T}_h)} \\
&\leqslant \|\widetilde{\mathcal{M}}_\rho(u_h - v_h - 0_h)\|_{L^2(\mathcal{T}_h)} + \|\widetilde{\mathcal{M}}_\rho 0_h\|_{L^2(\mathcal{T}_h)} \\
&\leqslant \Big(1 - \frac{\rho c}{2}\Big)\|u_h - v_h - 0_h\|_{L^2(\mathcal{T}_h)} + \|\widehat{0}_h\|_{L^2(\mathcal{T}_h)},
\end{aligned}$$

and it follows that

$$\|u_h - v_h\|_{L^2(\mathcal{T}_h)} \leqslant \frac{1}{1 - \Big(1 - \frac{\rho c}{2}\Big)}\|\widehat{0}_h\|_{L^2(\mathcal{T}_h)} = \frac{2}{\rho c}\|\widehat{0}_h\|_{L^2(\mathcal{T}_h)}. \tag{24}$$

Observe that, since the L^2 projection operator is bounded with respect to the norm $\|\cdot\|_{L^2(\mathcal{T}_h)}$ (with constant 2) and by the definition of v_h, there holds

$$\begin{aligned}
\|\widehat{0}_h\|_{L^2(\mathcal{T}_h)} &= \|0_h - \rho\widetilde{\mathcal{H}}_h[0_h]\|_{L^2(\mathcal{T}_h)} \\
&= \rho\|\mathcal{H}_h[v_h]\|_{L^2(\mathcal{T}_h)} \\
&= \rho\Big\|-\sigma_h\Delta_{h,g}v_h + J_{h,g}(v_h) + \theta_h v_h + \mathbb{P}_h^r\mathcal{H}(\widetilde{\nabla}_{h,g}v_h, v_h, \cdot)\Big\|_{L^2(\mathcal{T}_h)} \\
&= \rho\Big\|\theta_h v_h + \mathbb{P}_h^r\mathcal{H}(\widetilde{\nabla}_{h,g}v_h, v_h, \cdot)\Big\|_{L^2(\mathcal{T}_h)} \\
&\leqslant \rho\theta_h\|v_h\|_{L^2(\mathcal{T}_h)} + \rho\|\mathbb{P}_h^r\mathcal{H}(\widetilde{\nabla}_{h,g}v_h, v_h, \cdot) \\
&\quad - \mathbb{P}_h^r\mathcal{H}(\mathbf{0}, 0, \cdot)\|_{L^2(\mathcal{T}_h)} + \rho\|\mathbb{P}_h^r\mathcal{H}(\mathbf{0}, 0, \cdot)\|_{L^2(\mathcal{T}_h)} \\
&\leqslant \rho\theta_h\|v_h\|_{L^2(\mathcal{T}_h)} + \rho\kappa\|v_h\|_{L^2(\mathcal{T}_h)} \\
&\quad + \rho\kappa\sum_{i=1}^{d}\|\widetilde{\partial}_{h,x_i}^g v_h\|_{L^2(\mathcal{T}_h)} + \rho\|\mathbb{P}_h^r\mathcal{H}(\mathbf{0}, 0, \cdot)\|_{L^2(\mathcal{T}_h)} \\
&\leqslant \rho\big(\theta_h + (d+1)\kappa\big)C_1 + \rho 2\|\mathcal{H}(\mathbf{0}, 0, \cdot)\|_{L^2(\mathcal{T}_h)},
\end{aligned}$$

where we have used the fact that

$$\begin{aligned}
\|\widetilde{\partial}_{h,x_i}^g v_h\|_{L^2(\mathcal{T}_h)} \leqslant \frac{1}{4}\|\partial_{h,x_i}^{+,g} v_h\|_{L^2(\mathcal{T}_h)} + \frac{1}{4}\|\partial_{h,x_i}^{-,g} v_h\|_{L^2(\mathcal{T}_h)} \\
+ \frac{1}{4}\|\partial_{h,x_i}^{+} v_h\|_{L^2(\mathcal{T}_h)} + \frac{1}{4}\|\partial_{h,x_i}^{-} v_h\|_{L^2(\mathcal{T}_h)}.
\end{aligned}$$

Plugging this into (24), it follows that

$$\|u_h\|_{L^2(\mathcal{T}_h)} \leqslant \|v_h\|_{L^2(\mathcal{T}_h)} + \frac{2}{\rho c}\|\widehat{0}_h\|_{L^2(\mathcal{T}_h)} \leqslant \|v_h\|_{L^2(\mathcal{T}_h)} + \frac{2}{c}\Big(\big(\theta_h + (d+1)\kappa\big)C_1 + 2\|\mathcal{H}(\mathbf{0},0,\cdot)\|_{L^2(\mathcal{T}_h)}\Big),$$

and the result follows due to the assumption $\theta_h \to \theta > 0$.

Remark 6

(a) The requirement $\sigma_h > 0$ was used in the formation of v_h in (23). The stability analysis requires the presence of the vanishing viscosity, but the analysis is independent of the magnitude of σ_h allowing for the choice $\sigma_h \in \mathcal{O}(h^p)$ for any power p.

(b) Observe that the stability bound is inversely related to $\kappa_0 + \theta$ consistent with the standard stability estimates for (1). The analysis for the case $\kappa_0 = \theta = 0$ would require a new analytic technique or possibly more problem dependent techniques similar to the PDE theory when $\mathcal{H}(\mathbf{v}, v, x)$ is independent of v and $\theta = 0$.

5 Numerical Experiments

In this section we perform a series of experiments in two dimensions to gauge the effectiveness of (14) for approximating solutions to (1) and (10) for approximating solutions to (2). We consider the case $\theta > 0$ and the degenerate case $\theta = 0$. All problems will be computed on the domain $\Omega = (0,1)^2$ using a criss-cross mesh. The meshes are all uniform refinements of the coarse level mesh corresponding to an edge length of 1/2 along the boundary of the domain. The refinements use the uniform bisection method in the iFEM Matlab package and correspond to dividing each triangle into four triangles by placing a vertex at the midpoint of each edge. As such, the meshes are all quasi-uniform and have only one boundary edge. For $\sigma > 0$ in (10), the jump term $J_{h,g}$ is not necessary based on results for the DWDG method for Poisson's equation (see [23]). We perform most tests with $\gamma_e = 0$ for all $e \in \mathcal{E}_h$ to test whether the L^2 stability result is strong enough to eliminate the need for the jump term even with a vanishing viscosity stabilizer (as suggested by the results in Sect. 4). Overall, we observed analogous results for the choices $\gamma_e = 0$ for all $e \in \mathcal{E}_h$ and $\gamma_e = 1$ for all $e \in \mathcal{E}_h$. We will record the results for $\gamma_e \neq 0$ for one of the test problems. The lack of a penalty term is interesting because standard LDG methods for Poisson's equation are unstable on a criss-cross mesh without penalization. All errors correspond to absolute errors measured in the L^2 norm and H^1 semi-norm, where ∇u_h corresponds to the standard piecewise gradient operator defined over $\mathcal{T}_h$.

We initialize all solvers with the initial guess corresponding to the function $v_h(x) = 1$ on Ω. To solve (10), we simply use the *fsolve* command in Matlab. More care needs to be taken when solving (14) for $\sigma_h \in \mathcal{O}(h^p)$ for larger powers p. The pseudo-time stepping iteration (15) requires $\rho > 0$ with $\rho \in \mathcal{O}(h^2)$. As long as $c = \sigma_h\lambda + \theta_h + \kappa_0 \in \mathcal{O}(1)$ corresponding to $\theta > 0$ or $\kappa_0 > 0$, then the method is feasible. However, for $\theta_h \in \mathcal{O}(h^p)$, then the upper bound for the contraction constant is of the form $1 - Ch^{p+2}$ (or an appropriate constant C) which may be prohibitive for larger values of p. Numerical tests supported the observation that the pseudo-time stepping iteration converges too slowly to be practical based on the number of iterations needed for the solver to converge when using course meshes and $r = 1$. Instead, for all tests, we form a sequence of σ_h and θ_h values to generate a better

initial guess for *fsolve*. To this end, we choose a constant C and let $\sigma_h = \theta_h = Ch^p$. We then choose values $\sigma_k = \theta_k$ defined by $\sigma_k = Ch^{p_k}$ for $p = p_N > p_{N-1} > \cdots > p_2 > p_1 = 0$. Thus, the initial guess for *fsolve* is generated by first solving a sequence of regularized HJ equations. In the experiments, we choose a linear sequence of powers p_k. Such a strategy always worked for piecewise linear basis functions even with N small. For more degenerate cases, the solver sometimes could not find a solution when using piecewise quadratic and piecewise cubic basis functions. We did not test high-order polynomial bases on the finer meshes due to a lack of sufficient memory. Typically we could recover nearly optimal rates of convergence for $\theta_h = \theta + h^2$ and $\sigma_h = h^2$ when using piecewise linear basis functions. Rates for piecewise quadratic and piecewise cubic functions were more erratic.

All of the examples have a convex Hamilton yielding uniqueness for the viscosity solution. For most of the examples, the function $\mathcal{H}(\mathbf{v}, v, x)$ will be independent of v implying $\kappa_0 = 0$. We will approximate the problem for various choices of $\theta > 0$ and $\theta = 0$ to test how essential it is that $\max\{\kappa_0, \theta\} > 0$ since the restriction was necessary to prove stability in Theorem 2 and not admissibility in Theorem 1. Based on the theory for HJ equations, this is a potentially challenging case. The nonlinear examples that we consider will involve the non one-to-one term u_x^2 or $|u_x|$ in the definition of the operator $\mathcal{H}$. Since u_x could be positive or negative, there are likely false solutions in the degenerate case that would not correspond to the viscosity solution. Even though we have the unique existence of an approximation u_h when $\sigma_h > 0$ or $\theta_h > 0$, we expect small-residual wells that can trap the nonlinear solver. When setting $\sigma_h = \theta_h = 0$, *fsolve* could not find a solution or would find solutions with large errors further emphasizing the need for the stabilization terms. Amazingly, we could overcome the solver issue and degeneracy issue in many cases even for $\sigma_h, \theta_h \in \mathcal{O}(h^p)$ with $p > 1$ which goes beyond the Godunov barrier for monotone methods.

As a simple example to illustrate how difficult the problems can be, we consider the following one-dimensional problem:

$$\mathcal{H}(u_x) = \left|u_x\right| - 1 = 0 \quad \text{in } \Omega = (-1, 1)$$

with $u(-1) = u(1) = 0$. The problem has a unique viscosity solution $u(x) = |x| - 1$, and $v(x) = 1 - |x|$ is the unique viscosity solution of $-\mathcal{H}(u_x) = 0$. Observe that the problem has infinitely many almost everywhere solutions corresponding to continuous piecewise linear functions that have slope ± 1 for each piece. See [22] for a detailed look at this example and [8, 27] for similar examples. Using a monotone finite difference scheme such as the Lax-Friedrich's method, the scheme has a unique solution that converges to the viscosity solution $u(x)$ (see [2]). If we instead use the trivial finite difference method based on replacing u_x with the central difference quotient, we encounter false algebraic solutions as seen in Fig. 1 which used *fsolve* with the initial guess given by the zero function. The pairs of adjacent nodes have the same value (of either $2h$ or 0) while the neighboring pairs of adjacent nodes have the opposite value to ensure the central difference operator has magnitude 1. We hypothesize that for the test problems in this section involving u_x^2 or $|u_x|$, small residual wells exist that can trap a nonlinear solver when choosing σ_h, θ_h small similar to this example.

5.1 Test 1: a Linear Benchmark

We first benchmark the scheme by considering the linear problem

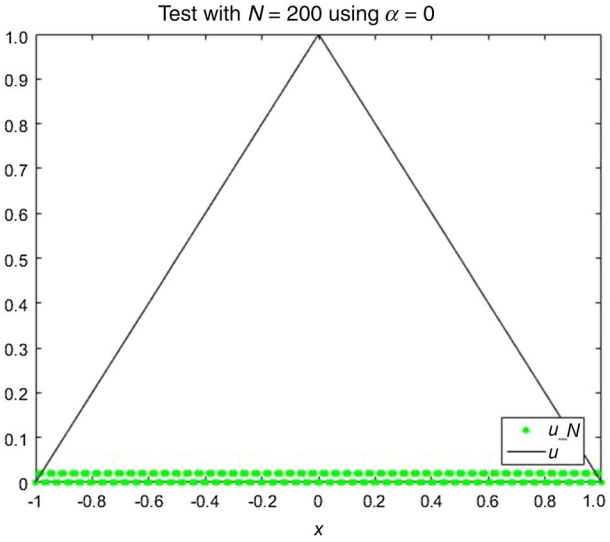

Fig. 1 An algebraic artifact when using a trivial finite difference method to approximate a viscosity solution

$$\begin{aligned} \mathcal{H}[u] \equiv -\sigma\Delta u + u_x + u_y + \theta u = f \qquad & \text{in } \Omega, \\ u = g \qquad & \text{on } \partial\Omega, \end{aligned}$$

where $\sigma \in \{0, 0.01, 1\}$ and $\theta \in \{0, 1, 10, 100\}$ with the data f and g chosen such that the exact solution is $u(x, y) = \mathrm{e}^{xy}$.

The first tests consider the regularized version corresponding to $\sigma \in \{0.01, 1\}$ and $\theta = 0$. By choosing $\sigma_h = \sigma + h^p$ we observe optimal rates of convergence in Table 1 when choosing $p = r + 1$. We note that we did not align fluxes to match the convection terms in the tests.

We next consider the non-regularized case by choosing $\sigma = 0$ and varying $\theta \in \{0, 1, 10, 100\}$. The results for piecewise linear basis functions with $\sigma_h = h^p$ and $\theta_h = \theta + h^p$ for $p = 1, 2$ can be found in Table 2. As $\theta \to 0^+$, the calculated rates appear to be either sub-optimal or in the pre-asymptotic range. The L^2 error rates overall increase as $h \to 0$, but they do not reach the same optimal levels recorded in Table 1 which used the stronger regularization based on adding a fixed diffusion term. The H^1 seminorm error rates are less consistent. Note that the last row corresponding to $\theta = 0$ is a degenerate case for which we cannot guarantee a strong L^2 stability estimate. While the calculated rates are suboptimal, the scheme does perform well even as the underlying problem transitions to degenerate.

5.2 Test 2: a Nonlinear $C^1 \setminus C^2$ Operator with Smooth Solution

We next consider the nonlinear problem

$$\begin{aligned} \mathcal{H}[u] \equiv -\sigma\Delta u + \sqrt{u_x^2 + u_y^2} + \theta u = f \quad & \text{in } \Omega, \\ u = g \quad & \text{on } \partial\Omega, \end{aligned}$$

Table 1 Results for Test 1 with $\sigma_h = \sigma + h^p$ for piecewise linear, piecewise quadratic, and piecewise cubic basis functions with no jump penalization

		$\sigma = 1$				$\sigma = 0.01$			
	h	$\|u - u_h\|_{L^2(\mathcal{T}_h)}$	Rate	$\|\nabla u - \nabla u_h\|_{L^2(\mathcal{T}_h)}$	Rate	$\|u - u_h\|_{L^2(\mathcal{T}_h)}$	Rate	$\|\nabla u - \nabla u_h\|_{L^2(\mathcal{T}_h)}$	Rate
Linear									
$p = 1$	1/2	7.887 0E–03	–	2.489 4E–01	–	1.767 3E–02	–	2.590 5E–01	–
	1/4	3.874 1E–03	1.026	1.261 9E–01	0.980	1.787 5E–02	−0.016	1.486 1E–01	0.802
	1/8	2.159 6E–03	0.843	6.372 3E–02	0.986	1.491 8E–02	0.261	9.276 1E–02	0.680
	1/16	1.152 4E–03	0.906	3.204 8E–02	0.992	1.023 8E–02	0.543	5.885 4E–02	0.656
	1/32	5.954 5E–04	0.953	1.607 3E–02	0.996	6.127 0E–03	0.741	3.653 0E–02	0.688
$p = 2$	1/2	6.862 7E–03	–	2.484 6E–01	–	1.687 0E–02	–	2.596 4E–01	–
	1/4	1.680 0E–03	2.030	1.250 9E–01	0.990	1.009 1E–02	0.741	1.351 2E–01	0.942
	1/8	4.083 4E–04	2.041	6.283 6E–02	0.993	3.349 4E–03	1.591	6.598 6E–02	1.034
	1/16	9.953 8E–05	2.036	3.151 9E–02	0.995	9.072 8E–04	1.884	3.232 6E–02	1.029
	1/32	2.444 3E–05	2.026	1.578 9E–02	0.997	2.319 2E–04	1.968	1.595 5E–02	1.019
Quad									
$p = 2$	1/2	4.141 5E–03	–	2.828 9E–02	–	1.834 8E–02	–	8.560 0E–02	–
	1/4	1.219 2E–03	1.764	7.590 6E–03	1.898	1.025 1E–02	0.840	4.911 9E–02	0.801
	1/8	3.191 7E–04	1.933	1.945 6E–03	1.964	3.379 6E–03	1.601	1.916 2E–02	1.358
	1/16	8.074 7E–05	1.983	4.905 8E–04	1.988	9.140 8E–04	1.886	6.277 2E–03	1.610
	1/32	2.024 7E–05	1.996	1.230 3E–04	1.995	2.332 9E–04	1.970	1.834 3E–03	1.775
$p = 3$	1/2	2.351 4E–03	–	2.336 5E–02	–	1.500 7E–02	–	7.047 1E–02	–
	1/4	3.242 2E–04	2.858	5.328 0E–03	2.133	3.379 8E–03	2.151	1.627 3E–02	2.115
	1/8	4.095 4E–05	2.985	1.303 7E–03	2.031	4.634 2E–04	2.867	2.641 2E–03	2.623
	1/16	5.119 7E–06	3.000	3.262 9E–04	1.998	5.864 9E–05	2.982	5.236 9E–04	2.334
	1/32	6.395 9E–07	3.001	8.186 8E–05	1.995	7.341 6E–06	2.998	9.993 5E–05	2.390
Cubic									
$p = 3$	1/2	2.290 1E–03	–	1.104 9E–02	–	1.498 7E–02	–	6.834 6E–02	–
	1/4	3.189 9E–04	2.844	1.529 6E–03	2.853	3.379 3E–03	2.149	1.898 3E–02	1.848
	1/8	4.045 1E–05	2.979	1.938 9E–04	2.980	4.633 5E–04	2.867	3.185 9E–03	2.575
	1/16	5.065 6E–06	2.997	2.428 0E–05	2.997	5.863 0E–05	2.982	4.727 2E–04	2.753
$p = 4$	1/2	1.216 8E–03	–	6.017 0E–03	–	1.024 8E–02	–	4.873 4E–02	–
	1/4	8.075 9E–05	3.913	4.290 9E–04	3.810	9.138 4E–04	3.487	4.559 3E–03	3.418
	1/8	5.067 0E–06	3.994	3.365 8E–05	3.672	5.863 0E–05	3.962	3.986 9E–04	3.515
	1/16	3.167 6E–07	4.000	3.267 0E–06	3.365	3.670 5E–06	3.998	2.990 7E–05	3.737

where $\sigma \in \{0, 0.01, 1\}$ and $\theta \in \{0, 1, 10, 100\}$ with the data f and g chosen such that the exact solution is $u(x, y) = \mathrm{e}^{xy}$.

The first tests consider the regularized version corresponding to $\sigma \in \{0.01, 1\}$ and $\theta = 0$. We again choose $\sigma_h = \sigma + h^p$. The results using linear, quadratic, and cubic basis functions can be found in Table 3. We see optimal rates for piecewise linear functions. Piecewise quadratic and piecewise linear basis functions do not yield optimal rates. The solver did not consistently find a solution using piecewise cubic functions with $\sigma = 0.01$ and $\sigma_h = \sigma + h^4$.

Table 2 Results for Test 1 with linear basis functions, $\sigma_h = h^p$, and $\theta_h = \theta + h^p$ with no jump penalization

		$p = 1$				$p = 2$			
	h	$\|u - u_h\|_{L^2(\mathcal{T}_h)}$	Rate	$\|\nabla u - \nabla u_h\|_{L^2(\mathcal{T}_h)}$	Rate	$\|u - u_h\|_{L^2(\mathcal{T}_h)}$	Rate	$\|\nabla u - \nabla u_h\|_{L^2(\mathcal{T}_h)}$	Rate
$\theta = 100$	1/2	3.991 0E–03	–	2.499 4E–01	–	2.555 9E–03	–	2.515 4E–01	–
	1/4	1.554 4E–03	1.360	1.252 4E–01	0.997	6.604 5E–04	1.952	1.263 4E–01	0.994
	1/8	7.230 6E–04	1.104	6.296 6E–02	0.992	2.564 2E–04	1.365	6.364 3E–02	0.989
	1/16	3.662 8E–04	0.981	3.169 0E–02	0.991	1.117 8E–04	1.198	3.259 2E–02	0.965
	1/32	1.882 7E–04	0.960	1.596 3E–02	0.989	4.427 8E–05	1.336	1.768 8E–02	0.882
$\theta = 10$	1/2	1.098 8E–02	–	2.519 6E–01	–	8.241 1E–03	–	2.514 9E–01	–
	1/4	7.395 1E–03	0.571	1.299 0E–01	0.955	2.858 1E–03	1.528	1.273 1E–01	0.982
	1/8	4.616 3E–03	0.679	6.757 0E–02	0.943	8.641 2E–04	1.726	6.540 4E–02	0.961
	1/16	2.659 1E–03	0.795	3.556 8E–02	0.925	8.838 0E–05	1.573	2.314 8E–02	0.624
	1/32	1.450 5E–03	0.874	1.913 1E–02	0.894	8.838 0E–05	1.573	2.314 8E–02	0.624
$\theta = 1$	1/2	1.677 8E–02	–	2.579 5E–01	–	1.535 0E–02	–	2.579 8E–01	–
	1/4	1.598 1E–02	0.070	1.444 2E–01	0.837	8.305 5E–03	0.886	1.328 6E–01	0.957
	1/8	1.264 3E–02	0.338	8.555 0E–02	0.755	2.679 6E–03	1.632	6.596 4E–02	1.010
	1/16	8.384 7E–03	0.592	5.097 7E–02	0.747	7.300 9E–04	1.876	3.468 5E–02	0.927
	1/32	4.925 0E–03	0.768	2.996 7E–02	0.766	1.992 1E–04	1.874	2.492 1E–02	0.477
$\theta = 0$	1/2	1.799 8E–02	–	2.595 1E–01	–	1.742 1E–02	–	2.605 6E–01	–
	1/4	1.846 7E–02	−0.037	1.500 7E–01	0.790	1.063 1E–02	0.713	1.363 9E–01	0.934
	1/8	1.559 8E–02	0.244	9.526 9E–02	0.656	3.560 0E–03	1.578	6.588 6E–02	1.050
	1/16	1.079 1E–02	0.531	6.200 8E–02	0.620	9.849 4E–04	1.854	3.797 6E–02	0.795
	1/32	6.497 8E–03	0.732	4.022 7E–02	0.624	2.841 9E–04	1.793	3.932 5E–02	−0.050

We next consider the non-regularized case by choosing $\sigma = 0$ and varying $\theta \in \{0, 1, 10, 100\}$. The results for piecewise linear basis functions with $\sigma_h = h^p$ and $\theta_h = \theta + h^p$ for $p = 1, 2$ can be found in Table 4. When $p = 2$ we see optimal rates for both the L^2 and H^1 errors for the smaller values of θ including the degenerate case.

5.3 Test 3: Nonlinear Lipschitz Operators with Smooth Solutions

We next consider the nonlinear problem

$$\begin{aligned} \mathcal{H}[u] \equiv -\sigma\Delta u + |u_x| + |u_y| + \theta u &= f \quad \text{in } \Omega, \\ u &= g \quad \text{on } \partial\Omega, \end{aligned}$$

where $\sigma \in \{0, 0.01, 1\}$ and $\theta \in \{0, 10, 50, 100, 250\}$ with the data f and g chosen such that the exact solution is $u(x, y) = \cos(\pi x)\cos(\pi y)$.

The first tests consider the regularized version corresponding to $\sigma \in \{0.01, 1\}$ and $\theta = 0$. We again choose $\sigma_h = \sigma + h^p$. The results using linear, quadratic, and cubic basis functions can be found in Table 5. We see optimal rates for piecewise linear functions. We also had surprisingly high rates of convergence in the H^1 seminorm when using piecewise linear basis functions with $p = 1$. Piecewise quadratic and piecewise linear basis functions do not yield optimal rates; however, the piecewise cubic functions behaved more optimally

Table 3 Results for Test 2 with $\sigma_h = \sigma + h^p$ for piecewise linear, piecewise quadratic, and piecewise cubic basis functions with no jump penalization

		$\sigma = 1$				$\sigma = 0.01$			
	h	$\|u - u_h\|_{L^2(\mathcal{T}_h)}$	Rate	$\|\nabla u - \nabla u_h\|_{L^2(\mathcal{T}_h)}$	Rate	$\|u - u_h\|_{L^2(\mathcal{T}_h)}$	Rate	$\|\nabla u - \nabla u_h\|_{L^2(\mathcal{T}_h)}$	Rate
Linear									
$p = 1$	1/2	7.752 6E–03	–	2.488 9E–01	–	1.678 9E–02	–	2.579 6E–01	–
	1/4	3.933 1E–03	0.979	1.261 6E–01	0.980	1.661 5E–02	0.015	1.462 3E–01	0.819
	1/8	2.196 8E–03	0.840	6.368 9E–02	0.986	1.403 9E–02	0.243	8.980 1E–02	0.703
	1/16	1.171 2E–03	0.907	3.202 3E–02	0.992	9.850 6E–03	0.511	5.550 5E–02	0.694
	1/32	6.048 5E–04	0.953	1.605 8E–02	0.996	5.961 1E–03	0.725	3.273 7E–02	0.762
$p = 2$	1/2	6.582 6E–03	1.830	2.482 9E–01	0.949	1.574 7E–02	–	2.579 8E–01	–
	1/4	1.664 0E–03	1.984	1.250 5E–01	0.990	9.736 7E–03	0.694	1.344 4E–01	0.940
	1/8	4.102 8E–04	2.020	6.282 8E–02	0.993	3.297 1E–03	1.562	6.597 6E–02	1.027
	1/16	1.004 8E–04	2.030	3.151 7E–02	0.995	8.946 2E–04	1.882	3.218 4E–02	1.036
	1/32	2.470 9E–05	2.024	1.578 9E–02	0.997	2.282 1E–04	1.971	1.589 2E–02	1.018
Quad									
$p = 2$	1/2	5.565 1E–03	–	3.290 6E–02	–	2.361 4E–02	–	1.113 0E–01	–
	1/4	2.251 5E–03	1.306	1.139 0E–02	1.531	1.847 1E–02	0.354	1.002 5E–01	0.151
	1/8	8.864 6E–04	1.345	4.186 9E–03	1.444	9.938 3E–03	0.894	8.215 4E–02	0.287
	1/16	3.725 8E–04	1.250	1.724 1E–03	1.280	4.455 9E–03	1.157	5.131 2E–02	0.679
	1/32	1.677 3E–04	1.151	7.781 2E–04	1.148	1.869 4E–03	1.253	2.482 4E–02	1.048
$p = 3$	1/2	4.036 4E–03	–	2.813 7E–02	–	–	–	–	–
	1/4	1.480 1E–03	1.447	8.637 1E–03	1.704	–	–	–	–
	1/8	6.472 4E–04	1.193	3.289 6E–03	1.393	–	–	–	–
	1/16	3.079 6E–04	1.072	1.480 2E–03	1.152	–	–	–	–
	1/32	1.510 7E–04	1.028	7.158 7E–04	1.048	–	–	–	–
Cubic									
$p = 3$	1/2	2.399 2E–03	–	1.158 0E–02	–	1.524 3E–02	–	6.921 8E–02	–
	1/4	3.596 7E–04	2.738	1.716 6E–03	2.754	3.874 4E–03	1.976	2.030 6E–02	1.769
	1/8	5.221 8E–05	2.784	2.465 9E–04	2.799	6.090 9E–04	2.669	3.866 4E–03	2.393
	1/16	8.210 6E–06	2.669	3.832 6E–05	2.686	9.722 9E–05	2.647	7.172 9E–04	2.430
$p = 4$	1/2	1.372 2E–03	–	6.703 5E–03	–	–	–	–	–
	1/4	1.314 4E–04	3.384	6.433 0E–04	3.381	–	–	–	–
	1/8	1.841 9E–05	2.835	8.888 4E–05	2.855	–	–	–	–
	1/16	3.704 6E–06	2.314	1.751 2E–05	2.344	–	–	–	–

in terms of rates for $\sigma = 1$. The solver did not consistently find a solution using piecewise cubic functions with $\sigma = 0.01$.

We next consider the non-regularized case by choosing $\sigma = 0$ and varying $\theta \in \{0, 10, 50, 100, 250\}$. The results for piecewise linear basis functions with $\sigma_h = h^p$ and $\theta_h = \theta + h^p$ for $p = 1, 2$ can be found in Table 6. When $p = 2$ we see optimal rates for both the L^2 and H^1 errors for the smaller values of θ including the degenerate case. For $p = 1$, we see the rates deteriorate as θ decreases towards the degenerate case.

We also consider another test in this section where the Hamiltonian is nonlinear with respect to the second argument u:

Table 4 Results for Test 2 with linear basis functions, $\sigma_h = h^p$, and $\theta_h = \theta + h^p$ with no jump penalization

		$p=1$				$p=2$			
	h	$\|u-u_h\|_{L^2(\mathcal{T}_h)}$	Rate	$\|\nabla u-\nabla u_h\|_{L^2(\mathcal{T}_h)}$	Rate	$\|u-u_h\|_{L^2(\mathcal{T}_h)}$	Rate	$\|\nabla u-\nabla u_h\|_{L^2(\mathcal{T}_h)}$	Rate
$\theta=100$	1/2	4.036 6E–03	–	2.498 0E–01	–	2.606 9E–03	–	2.512 9E–01	–
	1/4	1.553 5E–03	1.378	1.252 0E–01	0.997	6.023 6E–04	2.114	1.261 2E–01	0.995
	1/8	7.199 2E–04	1.110	6.295 5E–02	0.992	1.969 2E–04	1.613	6.337 3E–02	0.993
	1/16	3.645 3E–04	0.982	3.168 8E–02	0.990	8.451 4E–05	1.220	3.205 6E–02	0.983
	1/32	1.874 0E–04	0.960	1.596 0E–02	0.989	3.555 6E–05	1.249	1.674 0E–02	0.937
$\theta=10$	1/2	1.074 6E–02	–	2.516 4E–01	–	8.081 9E–03	–	2.508 1E–01	–
	1/4	7.122 1E–03	0.593	1.297 1E–01	0.956	2.743 0E–03	1.559	1.265 3E–01	0.987
	1/8	4.435 9E–03	0.683	6.751 8E–02	0.942	8.081 4E–04	1.763	6.415 2E–02	0.980
	1/16	2.558 8E–03	0.794	3.561 4E–02	0.923	2.369 7E–04	1.770	3.351 8E–02	0.937
	1/32	1.400 5E–03	0.870	1.921 4E–02	0.890	7.426 1E–05	1.674	1.938 1E–02	0.790
$\theta=1$	1/2	1.599 6E–02	–	2.570 0E–01	–	1.443 1E–02	–	2.565 3E–01	–
	1/4	1.491 8E–02	0.101	1.426 6E–01	0.849	7.911 8E–03	0.867	1.320 4E–01	0.958
	1/8	1.186 2E–02	0.331	8.363 4E–02	0.770	2.568 5E–03	1.623	6.605 5E–02	0.999
	1/16	7.948 9E–03	0.578	4.903 4E–02	0.770	6.948 3E–04	1.886	3.401 5E–02	0.957
	1/32	4.682 5E–03	0.763	2.777 3E–02	0.820	1.817 7E–04	1.935	1.901 8E–02	0.839
$\theta=0$	1/2	1.708 4E–02	–	2.583 7E–01	–	1.625 1E–02	–	2.587 8E–01	–
	1/4	1.716 7E–02	−0.007	1.475 4E–01	0.808	1.033 0E–02	0.654	1.360 7E–01	0.927
	1/8	1.473 2E–02	0.221	9.210 5E–02	0.680	3.535 0E–03	1.547	6.746 2E–02	1.012
	1/16	1.044 1E–02	0.497	5.810 0E–02	0.665	9.691 4E–04	1.867	3.365 5E–02	1.003
	1/32	6.356 2E–03	0.716	3.511 5E–02	0.726	2.521 2E–04	1.943	1.851 5E–02	0.862

$$\mathcal{H}[u] \equiv |u_x| + |u_y| + |u| + 2u = f \qquad \text{in } \Omega, \tag{25a}$$

$$u = g \quad \text{on } \partial\Omega, \tag{25b}$$

with the data f and g chosen such that the exact solution is $u(x,y) = \cos(\pi x)\cos(\pi y) - 0.5$. Note that the solution u changes sign over Ω ensuring $\mathcal{H}[u]$ is nonlinear with respect to u. The test results for piecewise linear basis functions with $\sigma_h = \theta_h = h^2$ can be found in Table 7. Note that the solver did not consistently find the solution for $r = 2$ but instead would get stuck in small-residual wells which *fsolve* reported was on the order of 10^{-6}.

5.4 Test 4: a Nonlinear Lipschitz Operator with a Lower-Regularity Solution

We lastly consider the nonlinear problem

$$\begin{aligned} \mathcal{H}[u] \equiv |u_x| + 2u_x + \theta u &= f \qquad \text{in } \Omega, \\ u &= g \qquad \text{on } \partial\Omega, \end{aligned}$$

where $\theta \in \{0, 10\}$ with the data f and g chosen such that the exact solution is $u(x,y) = |x - 0.2|$. Note that we have set $\sigma = 0$ for all tests and that while $\mathcal{H}$ is convex, the function f is only bounded instead of continuous since we would have

Table 5 Results for Test 3 with $\sigma_h = \sigma + h^p$ for piecewise linear, piecewise quadratic, and piecewise cubic basis functions with no jump penalization

		$\sigma = 1$				$\sigma = 0.01$			
	h	$\|u - u_h\|_{L^2(\mathcal{T}_h)}$	Rate	$\|\nabla u - \nabla u_h\|_{L^2(\mathcal{T}_h)}$	Rate	$\|u - u_h\|_{L^2(\mathcal{T}_h)}$	Rate	$\|\nabla u - \nabla u_h\|_{L^2(\mathcal{T}_h)}$	Rate
Linear									
$p = 1$	1/2	5.786 8E–02	–	8.959 8E–01	–	1.094 2E–01	–	1.103 1E+00	–
	1/4	2.600 6E–02	1.154	4.732 0E–01	0.921	9.386 4E–02	0.221	8.500 0E–01	0.376
	1/8	1.263 4E–02	1.041	2.420 7E–01	0.967	8.970 9E–02	0.065	7.483 3E–01	0.184
	1/16	6.220 7E–03	1.022	1.215 3E–01	0.994	7.622 1E–02	0.235	5.920 0E–01	0.338
	1/32	3.082 1E–03	1.013	6.066 3E–02	1.002	5.357 3E–02	0.509	4.068 2E–01	0.541
$p = 2$	1/2	4.753 4E–02	–	8.689 4E–01	–	1.096 4E–01	–	1.084 8E+00	–
	1/4	1.397 4E–02	1.766	4.380 0E–01	0.988	8.120 4E–02	0.433	6.768 2E–01	0.681
	1/8	3.742 8E–03	1.901	2.160 2E–01	1.020	3.393 3E–02	1.259	3.214 7E–01	1.074
	1/16	9.585 9E–04	1.965	1.070 6E–01	1.013	9.803 7E–03	1.791	1.340 2E–01	1.262
	1/32	2.417 0E–04	1.988	5.331 9E–02	1.006	2.564 4E–03	1.935	5.816 8E–02	1.204
Quad									
$p = 2$	1/2	9.153 2E–02	–	8.319 2E–01	–	2.079 5E–02	–	2.323 2E–01	–
	1/4	6.860 8E–02	0.416	6.231 7E–01	0.417	6.272 7E–03	1.729	6.651 8E–02	1.804
	1/8	2.688 0E–02	1.352	3.255 4E–01	0.937	2.073 4E–03	1.597	1.833 7E–02	1.859
	1/16	1.003 2E–02	1.422	1.556 1E–01	1.065	8.495 2E–04	1.287	5.570 0E–03	1.719
	1/32	4.450 7E–03	1.173	7.048 2E–02	1.143	4.013 1E–04	1.082	2.090 3E–03	1.414
$p = 3$	1/2	1.315 4E–02	–	1.876 4E–01	–	–	–	–	–
	1/4	3.333 4E–03	1.981	4.588 9E–02	2.032	–	–	–	–
	1/8	1.583 1E–03	1.074	1.291 6E–02	1.829	–	–	–	–
	1/16	7.956 7E–04	0.993	4.483 5E–03	1.526	–	–	–	–
	1/32	3.984 9E–04	0.998	1.919 2E–03	1.224	–	–	–	–
Cubic									
$p = 3$	1/2	1.083 0E–02	–	1.014 3E–01	–	8.923 5E–02	–	7.447 6E–01	–
	1/4	1.497 7E–03	2.854	1.414 8E–02	2.842	3.026 9E–02	1.560	2.498 0E–01	1.576
	1/8	1.897 5E–04	2.981	1.802 5E–03	2.973	4.676 1E–03	2.694	6.091 5E–02	2.036
	1/16	2.377 7E–05	2.996	2.266 1E–04	2.992	4.037 6E–03	0.212	7.060 0E–02	−0.213
$p = 4$	1/2	5.788 6E–03	–	5.639 9E–02	–	–	–	–	–
	1/4	3.955 1E–04	3.871	4.423 2E–03	3.672	–	–	–	–
	1/8	3.225 3E–05	3.616	4.214 6E–04	3.392	–	–	–	–
	1/16	3.536 2E–06	3.189	4.806 3E–05	3.132	–	–	–	–

$$f(x, y) = \begin{cases} -1 + \theta|x - 0.2|, & \text{if } x \leqslant 0.2, \\ 3 + \theta|x - 0.2|, & \text{if } x > 0.2. \end{cases}$$

In the definition of the viscosity solution, we would need to take the upper (respectively, lower) semicontinuous envelope of the function

$$\mathcal{H}^0(\mathbf{v}, v, x, y) = |v_1| + 2v_1 - f(x, y)$$

when defining a viscosity supersolution (respectively, subsolution). Clearly u satisfies the problem for all $x \neq 0.2$, and u cannot be touched from above by a C^1 function at

Table 6 Results for Test 3 with linear basis functions, $\sigma_h = h^p$, and $\theta_h = \theta + h^p$ with no jump penalization

		$p=1$				$p=2$			
	h	$\|u-u_h\|_{L^2(\mathcal{T}_h)}$	Rate	$\|\nabla u-\nabla u_h\|_{L^2(\mathcal{T}_h)}$	Rate	$\|u-u_h\|_{L^2(\mathcal{T}_h)}$	Rate	$\|\nabla u-\nabla u_h\|_{L^2(\mathcal{T}_h)}$	Rate
$\theta=250$	1/2	2.101 5E–02	–	8.312 1E–01	–	1.205 5E–02	–	8.401 7E–01	–
	1/4	9.567 1E–03	1.135	4.239 1E–01	0.971	2.891 0E–03	2.060	4.286 0E–01	0.971
	1/8	4.680 4E–03	1.031	2.150 9E–01	0.979	7.688 1E–04	1.911	2.157 0E–01	0.991
	1/16	2.371 2E–03	0.981	1.097 5E–01	0.971	2.445 8E–04	1.652	1.085 2E–01	0.991
	1/32	1.211 2E–03	0.969	5.652 0E–02	0.957	9.615 0E–05	1.347	5.532 6E–02	0.972
$\theta=100$	1/2	3.944 8E–02	–	8.315 5E–01	–	2.487 9E–02	–	8.292 7E–01	–
	1/4	1.964 8E–02	1.006	4.389 6E–01	0.922	6.516 9E–03	1.933	4.249 9E–01	0.964
	1/8	1.034 1E–02	0.926	2.321 6E–01	0.919	1.733 4E–03	1.911	2.149 0E–01	0.984
	1/16	5.494 1E–03	0.912	1.247 3E–01	0.896	5.086 7E–04	1.769	1.094 9E–01	0.973
	1/32	2.882 3E–03	0.931	6.822 6E–02	0.870	1.771 2E–04	1.522	5.823 8E–02	0.911
$\theta=50$	1/2	5.714 9E–02	–	8.618 3E–01	–	3.949 5E–02	–	8.321 9E–01	–
	1/4	3.153 9E–02	0.858	4.804 3E–01	0.843	1.156 6E–02	1.772	4.263 7E–01	0.965
	1/8	1.803 1E–02	0.807	2.718 8E–01	0.821	3.161 0E–03	1.871	2.160 7E–01	0.981
	1/16	1.005 8E–02	0.842	1.569 2E–01	0.793	8.875 0E–04	1.833	1.123 6E–01	0.943
	1/32	5.428 3E–03	0.890	9.153 9E–02	0.778	2.953 6E–04	1.587	6.295 9E–02	0.836
$\theta=10$	1/2	9.237 1E–02	–	1.005 7E+00	–	7.945 5E–02	–	9.404 4E–01	–
	1/4	6.622 5E–02	0.480	6.787 5E–01	0.567	3.472 8E–02	1.194	4.943 6E–01	0.928
	1/8	4.865 8E–02	0.445	4.960 5E–01	0.452	1.137 9E–02	1.610	2.437 9E–01	1.020
	1/16	3.226 3E–02	0.593	3.493 2E–01	0.506	3.382 0E–03	1.750	1.414 6E–01	0.785
	1/32	1.943 3E–02	0.731	2.342 7E–01	0.576	1.713 9E–03	0.981	7.986 2E–02	0.825
$\theta=0$	1/2	1.136 0E–01	–	1.106 4E+00	–	1.182 1E–01	–	1.083 9E+00	–
	1/4	1.030 5E–01	0.141	8.471 8E–01	0.385	8.336 3E–02	0.504	6.352 3E–01	0.771
	1/8	9.864 3E–02	0.063	6.945 8E–01	0.287	3.195 4E–02	1.383	2.934 9E–01	1.114
	1/16	7.799 4E–02	0.339	5.016 6E–01	0.469	9.207 1E–03	1.795	1.364 0E–01	1.106
	1/32	5.194 3E–02	0.586	3.210 7E–01	0.644	2.317 1E–03	1.990	6.849 3E–02	0.994
	1/64	3.109 6E–02	0.740	1.894 3E–01	0.761	5.321 0E–04	2.123	3.925 1E–02	0.803

Table 7 Results for (25) with linear basis functions and $\sigma_h = \theta_h = h^2$ with no jump penalization

h	$\|u-u_h\|_{L^2(\mathcal{T}_h)}$	Rate	$\|\nabla u-\nabla u_h\|_{L^2(\mathcal{T}_h)}$	Rate
1/2	1.163 1E–01	–	1.061 8E+00	–
1/4	7.307 4E–02	0.671	6.047 2E–01	0.812
1/8	2.680 9E–02	1.447	2.789 1E–01	1.116
1/16	7.457 9E–03	1.846	1.321 9E–01	1.077
1/32	1.860 3E–03	2.003	6.855 0E–02	0.947

$x = 0.2$. Suppose $\varphi \in C^1(\overline{\Omega})$ touches the graph of $u(x)$ from below at $x = 0.2$. Then $\varphi_x(0.2, y) \in [-1, 1]$, and we have $|\varphi_x(0.2, y)| + 2\varphi_x(0.2, y) + \theta\varphi(0.2, y) + \liminf_{(\xi,\eta)\to(0.2,y)} \big(-f(\xi, \eta)\big) = |\varphi_x(0.2, y)| + 2\varphi_x(0.2, y) + (-3) \leqslant 3 - 3 = 0$, and it follows that u is a viscosity solution.

The viscosity solution is only Lipschitz continuous, and the line $x = 0.2$ does not align with any of the meshes. We expect low rates of convergence due to the low regularity of the solution. The problem tests the ability of the methods to capture viscosity solutions of (1) with less regularity. We note that for $\theta_h = \theta = 10$ with $\sigma_h = 0$ and no jump penalization, *fsolve* only found a solution for the first two meshes. When letting $\theta_h = \theta = 0$ with $\sigma_h = 0$ and no jump penalization, *fsolve* only found a solution for the first two meshes, and theses solutions were far from the exact solution u implying the scheme likely has algebraic artifacts when the stabilizer terms are not present.

The results for $\theta = 10$ can be found in Table 8. The results for the degenerate case $\theta = 0$ can be found in Table 9. Overall, the rates are erratic with some levels showing improvement beyond what would be optimal and others showing no improvement after a mesh refinement. All cases use $\sigma_h = h^p$ and $\theta_h = \theta + h^p$ for various values of p. The solver was able to find a solution in all cases with $N = 3$. As expected, there is no real gain in accuracy when using higher order basis functions. We can see the presence of a possible boundary layer and the error along $x = 0.2$ in Fig. 2. It is not clear which is the larger source of error. We also see the potential for algebraic artifacts when we set $\sigma_h = \theta_h = 0$ in Fig. 2 indicating why the solvers can have trouble for $\sigma_h = \theta_h = h^p$ for p large.

6 Extensions and Improvements

In this section, we discuss how to improve the DWDG scheme defined by (10) or (14) to be more stable and robust as well as to increase the chance for being able to prove the convergence by incorporating ideas from [13, 38], and [11, 12]. To this end, we introduce three types of stabilization operators, namely, the numerical viscosity operator $V_h : \mathcal{V}_h \to V_h^r$, the numerical moment operator $M_h : \mathcal{V}_h \to V_h^r$, and the vanishing moment $\Delta_{h,0,g}^2 \equiv \Delta_{h,0}\Delta_{h,g} : \mathcal{V}_h \to V_h^r$ with V_h and M_h defined by

$$V_h \equiv -\sum_{i=1}^{d} \left(\partial_{h,x_i}^{+,g} - \partial_{h,x_i}^{-,g} \right), \qquad M_h \equiv \sum_{i=1}^{d} \left(\partial_{h,x_i}^{++,g} - \partial_{h,x_i}^{-+,g} - \partial_{h,x_i}^{+-,g} + \partial_{h,x_i}^{--,g} \right), \tag{26}$$

where $\partial_{h,x_i}^{\mu\nu,g} \equiv \partial_{h,x_i}^{\mu} \partial_{h,x_i}^{\nu,g}$ for $\mu, \nu \in \{-,+\}$. See Sect. 6.1 for more information about the numerical viscosity and Sect. 6.2 for more information about the numerical moment. The vanishing moment corresponds to adding a scaled moment operator paired with a simply supported boundary condition and represents a discrete form of the vanishing moment method discussed in [14]. Adding these stabilizers to the scheme defined by (10) or (14), we have the following modified scheme:

$$\begin{aligned} 0 = {} & \tau_h \Delta_{h,0,g}^2 u_h - \sigma_h \Delta_{h,g} u_h + \mathbb{P}_h^r \mathcal{H}(\widetilde{\nabla}_{h,g} u_h, u_h, x) \\ & + \theta_h u_h + J_{h,g}(u_h) + \alpha_h M_h u_h + \beta_h V_h u_h, \end{aligned} \tag{27}$$

where $\alpha_h, \beta_h, \tau_h \geqslant 0$. Clearly $\Delta_{h,0,0}^2$ is a symmetric positive definite operator. Based on the results in Sects. 6.1 and 6.2 below, we can immediately extend the results in Sect. 4 by making the observation that both $\alpha_h M_h$ and $\beta_h V_h$ are symmetric nonnegative definite operators. We now give a few remarks that provide more context for how our proposed schemes (10), (14), and (27) relate to the methods in [38] and [11, 12].

Remark 7

Table 8 Results for Test 4 with linear basis functions, $\sigma_h = h^p$, and $\theta_h = 10 + h^p$ with no jump penalization

Linear	h	$\|u - u_h\|_{L^2(\mathcal{T}_h)}$	Rate	$\|\nabla u - \nabla u_h\|_{L^2(\mathcal{T}_h)}$	Rate
$p = 1$	1/2	7.497 5E–02	–	6.312 5E–01	–
	1/4	5.449 1E–02	0.460	4.340 4E–01	0.540
	1/8	4.172 9E–02	0.385	3.917 1E–01	0.148
	1/16	2.705 7E–02	0.625	2.796 3E–01	0.486
	1/32	1.437 2E–02	0.913	2.172 5E–01	0.364
	1/64	8.060 7E–03	0.834	1.538 5E–01	0.498
$p = 2$	1/2	6.340 9E–02	–	5.910 5E–01	–
	1/4	2.374 5E–02	1.417	2.959 1E–01	0.998
	1/8	1.328 1E–02	0.838	3.457 1E–01	−0.224
	1/16	4.469 2E–03	1.571	1.723 4E–01	1.004
	1/32	1.197 8E–03	1.900	1.302 6E–01	0.404
$p = 3$	1/2	4.858 2E–02	–	5.442 6E–01	–
	1/4	6.948 7E–03	2.806	2.415 8E–01	1.172
	1/8	1.069 8E–02	−0.623	4.036 7E–01	−0.741
	1/16	3.741 6E–03	1.516	2.309 2E–01	0.806
	1/32	1.173 9E–03	1.672	1.892 9E–01	0.287
Quad					
$p = 2$	1/2	5.923 8E–02	–	4.640 1E–01	–
	1/4	2.116 6E–02	1.485	2.951 8E–01	0.653
	1/8	1.065 9E–02	0.990	2.659 5E–01	0.150
	1/16	3.273 3E–03	1.703	2.733 2E–01	−0.039
	1/32	1.123 9E–03	1.542	1.185 0E–01	1.206
$p = 3$	1/2	4.663 0E–02	–	4.264 9E–01	–
	1/4	7.562 1E–03	2.624	2.695 9E–01	0.662
	1/8	6.536 4E–03	0.210	5.371 3E–01	−0.995
	1/16	6.931 2E–03	−0.085	1.017 3E+00	−0.921
	1/32	1.475 2E–03	2.232	3.602 0E–01	1.498
Cubic					
$p = 3$	1/2	2.653 9E–02	–	3.955 5E–01	–
	1/4	4.849 5E–03	2.452	2.423 1E–01	0.707
	1/8	8.229 9E–03	−0.763	4.809 6E–01	−0.989
	1/16	1.483 3E–03	2.472	4.416 9E–01	0.123
	1/32	3.136 8E–03	−1.081	9.137 5E–01	−1.049
$p = 4$	1/2	1.520 2E–02	–	4.166 4E–01	–
	1/4	6.139 2E–03	1.308	3.853 9E–01	0.112
	1/8	8.590 4E–03	−0.485	8.771 9E–01	−1.187
	1/16	2.427 3E–03	1.823	7.056 1E–01	0.314
	1/32	3.750 9E–03	−0.628	1.252 5E+00	−0.828

(a) If $\widetilde{\nabla}_{h,g} u_h$ is replaced with $\overline{\nabla}_{h,g} u_h$ in (14), then for $\beta_h > 0$ sufficiently large and $\sigma_h = \gamma_e = \alpha_h = \tau_h = 0$ and $\theta_h = \theta$, it can be shown that the method reduces to a scheme which is equivalent to Yan-Osher's LDG scheme formulated for time-dependent HJ equations in [38]. See [17] for details.

Table 9 Results for Test 4 with $\theta = 0$ and $\sigma_h = \theta_h = h^p$

		$\gamma_e = 0$				$\gamma_e = 1$			
	h	$\|u - u_h\|_{L^2(\mathcal{T}_h)}$	Rate	$\|\nabla u - \nabla u_h\|_{L^2(\mathcal{T}_h)}$	Rate	$\|u - u_h\|_{L^2(\mathcal{T}_h)}$	Rate	$\|\nabla u - \nabla u_h\|_{L^2(\mathcal{T}_h)}$	Rate
Linear									
$p = 1$	1/2	1.190 7E–01	–	7.525 1E–01	–	1.196 0E–01	–	7.581 0E–01	–
	1/4	1.153 0E–01	0.046	6.312 6E–01	0.253	1.159 7E–01	0.044	6.359 2E–01	0.254
	1/8	1.047 3E–01	0.139	6.039 6E–01	0.064	1.045 6E–01	0.149	6.034 8E–01	0.076
	1/16	7.336 4E–02	0.513	4.827 9E–01	0.323	7.353 2E–02	0.508	4.832 4E–01	0.321
	1/32	3.708 1E–02	0.984	3.380 0E–01	0.514	3.688 3E–02	0.995	3.366 5E–01	0.521
	1/64	1.947 0E–02	0.929	2.373 0E–01	0.510	1.942 5E–02	0.925	2.371 7E–01	0.505
$p = 2$	1/2	1.281 8E–01	–	7.578 8E–01	–	1.297 9E–01	–	7.702 9E–01	–
	1/4	6.930 7E–02	0.887	4.110 0E–01	0.883	7.621 9E–02	0.768	4.445 8E–01	0.793
	1/8	2.721 4E–02	1.349	3.818 8E–01	0.106	2.384 1E–02	1.677	3.910 3E–01	0.185
	1/16	9.981 2E–03	1.447	2.061 2E–01	0.890	7.261 1E–03	1.715	1.897 4E–01	1.043
	1/32	2.666 0E–03	1.905	1.438 8E–01	0.519	5.767 0E–04	3.654	1.385 3E–01	0.454
	1/64	1.564 6E–04	4.091	6.664 6E–02	1.110	1.723 1E–04	1.743	8.625 1E–02	0.684
Quad									
$p = 2$	1/2	1.263 1E–01	–	6.868 7E–01	–	1.264 5E–01	–	6.867 2E–01	–
	1/4	5.835 6E–02	1.114	4.265 9E–01	0.687	5.821 7E–02	1.119	4.248 2E–01	0.693
	1/8	2.439 3E–02	1.258	3.118 3E–01	0.452	2.462 1E–02	1.242	3.041 1E–01	0.482
	1/16	5.393 6E–03	2.177	3.027 5E–01	0.043	4.025 7E–03	2.613	2.857 6E–01	0.090
	1/32	2.330 4E–03	1.211	1.274 8E–01	1.248	9.099 5E–04	2.145	1.339 1E–01	1.094
$p = 3$	1/2	1.183 1E–01	–	6.583 1E–01	–	1.188 3E–01	–	6.572 9E–01	–
	1/4	1.550 7E–02	2.932	3.102 4E–01	1.085	1.473 1E–02	3.012	3.138 5E–01	1.066
	1/8	9.783 9E–03	0.664	5.904 4E–01	−0.928	6.217 5E–03	1.244	6.655 7E–01	−1.085
	1/16	1.394 2E–02	−0.511	1.833 9E+00	−1.635	1.221 2E–02	−0.974	1.545 7E+00	−1.216
	1/32	2.526 0E–03	2.464	4.968 1E–01	1.884	1.131 9E–03	3.432	2.649 4E–01	2.544
Cubic									
$p = 3$	1/2	5.986 8E–02	–	4.967 1E–01	–	5.983 4E–02	–	4.958 4E–01	–
	1/4	8.028 7E–03	2.899	2.565 4E–01	0.953	8.296 1E–03	2.850	2.469 1E–01	1.006
	1/8	1.623 3E–02	−1.016	6.423 3E–01	−1.324	1.382 6E–02	−0.737	6.056 2E–01	−1.294
	1/16	1.806 4E–03	3.168	4.708 2E–01	0.448	2.104 8E–03	2.716	4.996 1E–01	0.278
	1/32	6.775 3E–03	−1.907	1.755 9E+00	−1.899	7.199 7E–03	−1.774	1.130 3E+00	−1.178

(b) If $\widetilde{\nabla}_{h,g} u_h$ is replaced with $\overline{\nabla}_{h,g} u_h$, then for $\alpha_h > 0$, $\sigma > 0$, and $\tau_h = 0$, it can be shown that the method (10) is a special case of the nonstandard LDG method proposed by the first two authors in [11, 12] for fully nonlinear second order problems. See [11, 12] and [17] for details. The equivalence requires choosing the numerical moment coefficient matrix to be diagonal.

(c) The LDG schemes in [38] and [12] both use $\overline{\nabla}_{h,g}$ instead of $\widetilde{\nabla}_{h,g}$ inside $\mathcal{H}$. As seen by (7), this would lead to an extra boundary term in (21) that is proportional to ρ instead of ρ^2. This would require more attention in finding a way to bound the extra terms. There is potential that sufficiently large boundary penalization in the operator $J_{h,g}$ could absorb this unsigned term, but depending on the necessary scaling, the formal truncation error may suffer. For quasi-uniform meshes and $\sigma > 0$, the DWDG Laplacian operator $-\Delta_{h,g}$ can control boundary terms scaled by $1/h_e$ as seen in [23], but it is not

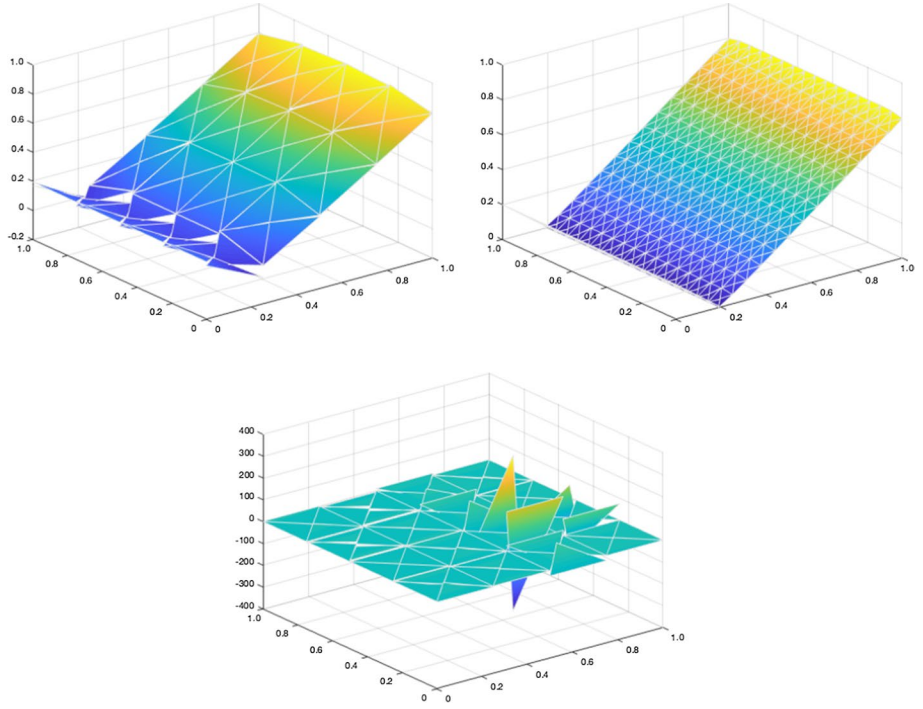

Fig. 2 Plots of the approximation u_h for Test 4 with $r = 1$, $\theta = 0$, and $\sigma_h = \theta_h = h^2$. The top left plot is for $h = 1/4$ and the top right plot is for $h = 1/16$. Note that there is some curvature along the boundary nodes coming from the interior. The bottom plot is a false solution for the case $\sigma_h = \theta_h = 0$. The residual recorded by *fsolve* was on the order of 10^{-29} for the false solution

immediately clear that the scaling would be sufficient to bound the extra terms. More work would need to be done on this front to potentially expand the techniques in this paper to the choice $\overline{\nabla}_{h,g}$ instead of $\widetilde{\nabla}_{h,g}$ inside $\mathcal{H}$.

(d) For degenerate problems with $\kappa_0 = \theta = 0$, we see that the vanishing viscosity operator $-\sigma_h \Delta_{h,g}$ is stronger than the numerical viscosity operator $\beta_h V_h$ in providing a way to approximate solutions to (1). This is in direct contrast to FD methods where the two operators would be equivalent (as can be seen by the Lax-Friedrich's method). We similarly expect the vanishing moment operator to be stronger than the numerical moment operator in the DG setting despite the fact that the two are equivalent in the FD setting (see [13]).

6.1 The Numerical Viscosity

The numerical viscosity V_h defined by (26) is key for designing monotone finite difference methods such as the Lax-Friedrich's method (see [33]). The term also appears in Yan-Osher's LDG scheme in [38] that directly adapts the corresponding monotone finite difference scheme to the DG setting for dynamic HJ equations. The Yan-Osher's LDG scheme was shown numerically to be able to achieve high-order, but the admissibility and stability analysis for stationary problems was not addressed.

For a fixed $i \in \{1, 2, \cdots, d\}$, by (i) and (ii) of Definition 2, there holds

$$\begin{aligned}\left(\partial^{+,g}_{h,x_i}v_h-\partial^{-,g}_{h,x_i}v_h,w_h\right)_{\mathcal{T}_h}&=-\left\langle \mathcal{Q}_i^+(v_h)n^{(i)}-\mathcal{Q}_i^-(v_h)n^{(i)},[w]\right\rangle_{\mathcal{E}_h^{\mathrm{I}}}\\&=-\left\langle \mathrm{sgn}(n^{(i)})n^{(i)}[v_h],[w]\right\rangle_{\mathcal{E}_h^{\mathrm{I}}}\\&=-\left\langle |n^{(i)}|[v_h],[w]\right\rangle_{\mathcal{E}_h^{\mathrm{I}}}.\end{aligned}\tag{28}$$

Thus, the numerical viscosity operator $\beta_h V_h=-\beta\sum_{i=1}^d\left(\partial^{+,g}_{h,x_i}-\partial^{-,g}_{h,x_i}\right)$ is symmetric and nonnegative definite for all $\beta_h\geqslant 0$, and it can be absorbed into the operator $J_{h,g}$ for particular choices of γ_e. Furthermore, the numerical viscosity has a nontrivial nullspace containing all functions in $V_h^r\cap C^0(\Omega)$.

Remark 8 For finite difference methods, the numerical viscosity V_h corresponds to the scaled discrete Laplacian operator $-h\Delta_{h,0}u_h$. Analogously, for the piecewise constant DG space, there is no C^0 subspace consistent with the singularity of the numerical viscosity operator. We see that for $r\geqslant 1$, the numerical viscosity is no longer non-singular. As such, the numerical viscosity alone is not strong enough to ensure the admissibility and stability of the scheme using the analysis technique in Sect. 4.

6.2 The Numerical Moment

A numerical moment operator similar to M_h defined by (26) was used in [13, 15] to design convergent non-monotone finite difference methods for fully nonlinear elliptic PDEs. In the finite difference setting, the term is so named because it is equivalent to the scaled discrete biharmonic operator $h^2\Delta_{h,0}\Delta_{h,0}$. The DG analogs were formulated and tested in [11, 12]. Furthermore, it was shown in [12] that the numerical moment is equivalent to the jump operator $\alpha_h\sum_{i=1}^d\left\langle[\partial^{+,0}_{h,x_i}u_h-\partial^{-,0}_{h,x_i}u_h],[w_h]|n_e^{(i)}|\right\rangle_{\mathcal{E}_h^{\mathrm{I}}}$.

For a fixed $i\in\{1,2,\cdots,d\}$, notice that, by (6), there holds

$$\begin{aligned}&\left(\left(\partial^{++,g}_{h,x_i}-\partial^{-+,g}_{h,x_i}-\partial^{+-,g}_{h,x_i}+\partial^{--,g}_{h,x_i}\right)u_h,w_h\right)_{\mathcal{T}_h}\\=&\left(\left(\partial^{++,0}_{h,x_i}-\partial^{-+,0}_{h,x_i}-\partial^{+-,0}_{h,x_i}+\partial^{--,0}_{h,x_i}\right)u_h,w_h\right)_{\mathcal{T}_h}\\=&-\left(\left(\partial^{+}_{h,x_i}-\partial^{-}_{h,x_i}\right)\left(\partial^{-,0}_{h,x_i}-\partial^{+,0}_{h,x_i}\right)u_h,w_h\right)_{\mathcal{T}_h}\\=&\left(\left(\partial^{-,0}_{h,x_i}-\partial^{+,0}_{h,x_i}\right)u_h,\left(\partial^{-,0}_{h,x_i}-\partial^{+,0}_{h,x_i}\right)w_h\right)_{\mathcal{T}_h},\end{aligned}$$

and it follows that the numerical moment is symmetric nonnnegative definite. Furthermore, any function in $V_h^r\cap H^1(\Omega)$ is in the nullspace of the numerical moment since $\partial^{-,0}_{h,x_i}v_h=\partial^{+,0}_{h,x_i}v_h$ for all $v_h\in V_h^r\cap H^1(\Omega)$. Again, for the piecewise constant DG space on a rectangular mesh, we recover the finite difference numerical moment which is a stronger operator in the sense that it is strictly symmetric positive definite. This is the inspiration for adding $\tau_h\Delta^2_{h,0,g}u_h$ in (27) when considering bases for V_h^r with $r\geqslant 1$.

7 Conclusion

We have formulated some DWDG methods for approximating viscosity solutions of stationary HJ equations with Dirichlet boundary conditions that incorporate a natural stabilization term based on the vanishing viscosity method and a new skew-symmetric discrete derivative operator. The new schemes were proved to admit unique L^2 stable solutions when approximating non-degenerate problems. Furthermore, it was shown that the stability does not depend on the scaling of the vanishing viscosity term. As such, the schemes formally can have an optimal consistency error. Indeed, almost all of the numerical tests indicated optimal convergence rates for piecewise linear basis functions, and for the linear test problem in Sect. 5.1, optimal rates were also observed for higher-order basis functions. The admissibility and stability analysis provides a new approach for analyzing approximation schemes for stationary problems. Since the proposed DWDG methods are not monotone, the convergence framework of Barles and Souganidis in [2] does not apply. We look to develop new analysis techniques for proving the convergence of the numerical solution to the viscosity solution of the underlying HJ problem in forthcoming works.

References

1. Ayuso, B., Marini, L.D.: Discontinuous Galerkin methods for advection-diffusion-reaction problems. SIAM J. Numer. Anal. **47**, 1391–1420 (2009)
2. Barles, G., Souganidis, P.E.: Convergence of approximation schemes for fully nonlinear second order equations. Asympt. Anal. **4**, 271–283 (1991)
3. Barth, T.J., Sethian, J.A.: Numerical schemes for the Hamilton-Jacobi and level set equations on triangulated domains. J. Comp. Phys. **145**, 1–40 (1998)
4. Brenner, S.C., Scott, L.R.: The Mathematical Theory of Finite Element Methods, 3rd edn. Springer, Berlin (2008)
5. Brooks, A.N., Huges, T.J.: Streamline upwind/Petrov-Galerkin formulations for convection dominated flows with particular emphasis on the incompressible Navier-Stokes equations. Comput. Methods Appl. Mech. Engrg. **32**, 199–259 (1982)
6. Ciarlet, P.G.: The Finite Element Method for Elliptic Problems. North-Holland, Amsterdam (1978)
7. Cockburn, B., Dong, B.: An analysis of the minimal dissipation local discontinuous Galerkin method for convection-diffusion problems. J. Sci. Comput. **32**, 233–262 (2007)
8. Crandall, M.G., Lions, P.-L.: Viscosity solutions of Hamilton-Jacobi equations. Trans. Am. Math. Soc. **277**, 1–42 (1983)
9. Crandall, M.G., Lions, P.-L.: Two approximations of solutions of Hamilton-Jacobi equations. Math. Comp. **43**, 1–19 (1984)
10. Crandall, M.G., Ishii, H., Lions, P.-L.: User's guide to viscosity solutions of second order partial differential equations. Bull. Am. Math. Soc. **27**, 1–67 (1992)
11. Feng, X., Lewis, T.: Local discontinuous Galerkin methods for one-dimensional second order fully nonlinear elliptic and parabolic equations. J. Sci. Comput. **59**, 129–157 (2014)
12. Feng, X., Lewis, T.: Nonstandard local discontinuous Galerkin methods for fully nonlinear second order elliptic and parabolic equations in high dimensions. J. Sci. Comput. **77**, 1534–1565 (2018)
13. Feng, X., Lewis, T.: A narrow-stencil finite difference method for approximating viscosity solutions of Hamilton-Jacobi-Bellman equations. SIAM J. Numer. Anal. **59**(2), 886–924 (2021)
14. Feng, X., Neilan, M.: The vanishing moment method for fully nonlinear second order partial differential equations: formulation, theory, and numerical analysis, arXiv:1109.1183 [math.NA]
15. Feng, X., Kao, C., Lewis, T.: Convergent finite difference methods for one-dimensional fully nonlinear second order partial differential equations. J. Comput. Appl. Math. **254**, 81–98 (2013)
16. Feng, W., Lewis, T.L., Wise, S.M.: Discontinuous Galerkin derivative operators with applications to second-order elliptic problems and stability. Math. Meth. Appl. Sci. **38**, 5160–5182 (2015)

17. Feng, X., Lewis, T., Neilan, M.: Discontinuous Galerkin finite element differential calculus and applications to numerical solutions of linear and nonlinear partial differential equations. J. Comput. Appl. Math. **299**, 68–91 (2016)
18. Hu, C., Shu, C.-W.: A discontinuous Galerkin finite element method for Hamilton-Jacobi equations. SIAM J. Sci. Comp. **21**, 666–690 (1999)
19. Huang, S.-C., Wang, S., Teo, K.L.: Solving Hamilton-Jacobi-Bellman equations by a modified method of characteristics. Nonlinear Anal. **40**, 279–293 (2000)
20. Hughes, T.J.R., Franca, L.P., Hulbert, G.M.: A new finite element formulation for computational fluid dynamics: VIII. The Galerkin/least-squares method for advective-diffusive equations. Comput. Methods Appl. Mech. Engrg. **73**, 173–189 (1989)
21. Kao, C.Y., Osher, S., Qian, J.: Lax-Friedrichs sweeping scheme for static Hamilton-Jacobi equations. J. Comput. Phys. **196**, 367–391 (2004)
22. Katzourakis, N.: An Introduction to Viscosity Solutions for Fully Nonlinear PDE with Applications to Calculus of Variations in L^∞, SpringerBriefs in Mathematics. Springer, Cham (2015)
23. Lewis, T., Neilan, M.: Convergence analysis of a symmetric dual-wind discontinuous Galerkin method. J. Sci. Comput. **59**, 602–625 (2014)
24. Lewis, T., Rapp, A., Zhang, Y.: Convergence analysis of symmetric dual-wind discontinuous Galerkin approximation methods for the obstacle problem. J. Math. Anal. Appl. (2020). https://doi.org/10.1016/j.jmaa.2020.123840
25. Li, F., Shu, C.-W.: Reinterpretation and simplified implementation of a discontinuous Galerkin method for Hamilton-Jacobi equations. Appl. Math. Lett. **18**, 1204–1209 (2005)
26. Li, F., Yakovlev, S.: A central discontinuous Galerkin method for Hamilton-Jacobi equations. J. Sci. Comput. **45**, 404–428 (2010)
27. Lions, P.-L.: Generalized Solutions of Hamilton-Jacobi Equations. Pitman, London (1982)
28. Osher, S., Fedkiw, R.: Level Set Methods and Dynamic Implicit Surfaces. Applied Mathematical Sciences, vol. 153. Springer-Verlag, New York (2003)
29. Osher, S., Shu, C.-W.: High-order essentially nonoscillatory schemes for Hamilton-Jacobi equations. SIAM J. Numer. Anal. **28**, 907–922 (1991)
30. Rudin, W.: Functional Analysis. McGraw-Hill, New York (1991)
31. Sethian, J.A.: Level Set Methods and Fast Marching Methods: Evolving Interfaces in Computational Geometry, Fluid Mechanics, Computer Vision, and Materials Science, volume 3 of Cambridge Monographs on Applied and Computational Mathematics. 2nd ed. Cambridge University Press, Cambridge (1999)
32. Sethian, J.A., Vladimirsky, A.: Ordered upwind methods for static Hamilton-Jacobi equations: theory and algorithms. SIAM J. Numer. Anal. **41**, 325–363 (2003)
33. Shu, C.-W.: High order numerical methods for time dependent Hamilton-Jacobi equations. In: Mathematics and Computation in Imaging Science and Information Processing, Vol. 11 of Lect. Notes Ser. Inst. Math. Sci. Natl. Univ. Singap., World Sci. Publ., Hackensack, NJ, 2007, pp. 47–91 (2007)
34. Tadmor, E.: Approximate solutions of nonlinear conservation laws and related equations. Available at https://home.cscamm.umd.edu/people/faculty/tadmor/pub/PDEs/Tadmor.Lax+Nirenberg-97.pdf (1997)
35. Tadmor, E.: The numerical viscosity of entropy stable schemes for systems of conservation laws, I. Math. Comp. **49**, 91–103 (1987)
36. Tsai, Y.R., Cheng, L.-T., Osher, S., Zhao, H.K.: Fast sweeping algorithms for a class of Hamilton-Jacobi equations. SIAM J. Numer. Anal. **41**, 673–694 (2003)
37. Van der Vegt, J.J.W., Xia, Y., Xu, Y.: Positivity preserving limiters for time-implicit higher order accurate discontinuous Galerkin discretizations. SIAM J. Sci. Comput. **41**, 2037–2063 (2019)
38. Yan, J., Osher, S.: Direct discontinuous local Galerkin methods for Hamilton-Jacobi equations. J. Comp. Phys. **230**, 232–244 (2011)